https://doi.org/10.1093/plcell/koad310 THE PLANT CELL 2024: 36: 1119–1139

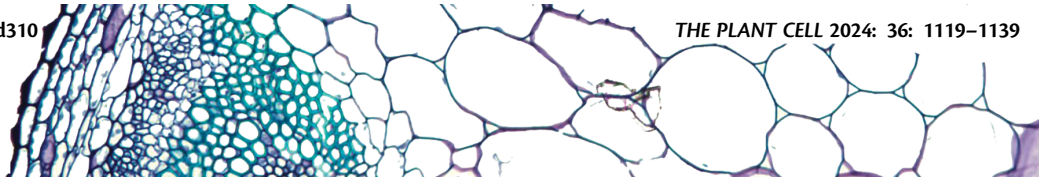

Research Article

UMAMIT44 is a key player in glutamate export from Arabidopsis chloroplasts

Samantha Vivia The [1], James P. Santiago [1], Clara Pappenberger [2], Ulrich Z. Hammes [2] and Mechthild Tegeder [1,*]

1 School of Biological Sciences, Washington State University, Pullman, WA, 99164, USA
2 Plant Systems Biology, School of Life Sciences Weihenstephan, Technical University of Munich, 85354 Freising, Germany

*Author for correspondence: tegeder@wsu.edu
The author responsible for distribution of materials integral to the findings presented in this article in accordance with the policy described in the Instructions for Authors (https://academic.oup.com/plcell/pages/General-Instructions) is: Mechthild Tegeder (tegeder@wsu.edu).

Abstract

Selective partitioning of amino acids among organelles, cells, tissues, and organs is essential for cellular metabolism and plant growth. Nitrogen assimilation into glutamine and glutamate and de novo biosynthesis of most protein amino acids occur in chloroplasts; therefore, various transport mechanisms must exist to accommodate their directional efflux from the stroma to the cytosol and feed the amino acids into the extraplastidial metabolic and long-distance transport pathways. Yet, Arabidopsis (*Arabidopsis thaliana*) transporters functioning in plastidial export of amino acids remained undiscovered. Here, USUALLY MULTIPLE ACIDS MOVE IN AND OUT TRANSPORTER 44 (UMAMIT44) was identified and shown to function in glutamate export from Arabidopsis chloroplasts. UMAMIT44 controls glutamate homeostasis within and outside of chloroplasts and influences nitrogen partitioning from leaves to sinks. Glutamate imbalances in chloroplasts and leaves of *umamit44* mutants impact cellular redox state, nitrogen and carbon metabolism, and amino acid (AA) and sucrose supply of growing sinks, leading to negative effects on plant growth. Nonetheless, the mutant lines adjust to some extent by upregulating alternative pathways for glutamate synthesis outside the plastids and by mitigating oxidative stress through the production of other amino acids and antioxidants. Overall, this study establishes that the role of UMAMIT44 in glutamate export from chloroplasts is vital for controlling nitrogen availability within source leaf cells and for sink nutrition, with an impact on growth and seed yield.

Introduction

Amino acids play a crucial role in the intricate metabolic networks of plants, which span across various compartments within cells. They are the basic constituents of peptides, proteins, and enzymes and act as precursors or nitrogen (N) donors for the biosynthesis of thousands of other compounds fundamental to plant growth and stress response (Tegeder and Masclaux-Daubresse 2018; Maeda 2019; Wang et al. 2019; Huang and Dudareva 2023). Plastids, and especially chloroplasts of photosynthetically active source leaves, serve as the site of N assimilation and they are also the major location of de novo synthesis of most proteinogenic amino acids. Since (i) all biochemical pathways require the action or presence of amino acids, (ii) amino acids serve as long-distance N transport forms from leaves to sinks (e.g. developing leaves and seeds) (Tegeder and Hammes 2018), and (iii) amino acids function as important signaling molecules in plant physiological processes and tolerance to abiotic and biotic stresses (Szabados and Savouré 2010; Toyota et al. 2018; Heinemann and Hildebrandt 2021), it is essential to understand how specific amino acids are fed into diverse metabolic pathways that are competing for N, and how this allocation is regulated.

To sustain the function of extra plastidial biochemical pathways, chloroplast-synthesized amino acids need first to be exported from the stroma to the cytosol across the envelope membranes. While the outer envelope membrane allows nonspecific movement of amino acids and amines through the OUTER ENVELOPE PORIN 16 (OEP16) channel (Pohlmeyer et al. 1997; Steinkamp et al. 2000), the inner

Received July 31, 2023. Accepted November 15, 2023. Advance access publication December 13, 2023

IN A NUTSHELL

Background: Plants produce amino acids in chloroplasts, and membrane transporters are needed to move these amino acids to the cytosol. In the cytosol, the amino acids are used for protein production and other biochemical pathways within leaf cells and to supply nitrogen to growing sink organs, such as seeds. However, despite their importance, little is known about these plastidial exporters.

Questions: What is the role of chloroplast amino acid (AA) transporters in leaf metabolism and long-distance transport of nitrogen? What is their physiological importance?

Findings: We found that *Arabidopsis thaliana* USUALLY MULTIPLE ACIDS MOVE IN AND OUT TRANSPORTER 44 (UMAMIT44) localizes to the chloroplast envelope and regulates plastidial glutamate export and glutamate homeostasis within and outside of chloroplasts. Decreased export and subsequent cellular imbalances in *umamit44* mutants impact the cellular redox state and affect both leaf nitrogen and carbon metabolism as well as the long-distance delivery of nitrogen and carbon to growing organs. Observed changes lead to decreased mutant growth and seed yield. Nevertheless, *umamit44* plants adapt to some extent by accelerating alternative pathways for glutamate synthesis outside of chloroplasts and by producing other amino acids and antioxidants to alleviate oxidative stress. Overall, we demonstrate that UMAMIT44 is an essential player in plastidial glutamate export and vital for plant growth and development.

Next steps: Transcriptome, $^{13}CO_2$ labeling, and metabolic flux analyses are needed to determine the interrelationship between plastidial AA export, cellular metabolism, and sink nitrogen supply. In addition, the identification of further chloroplast AA transport systems is a "must-do" as our understanding of the kind of transporters that mediate chloroplast efflux or influx of amino acids, and how they affect metabolic networks, metabolite levels, and sink nitrogen nutrition, remains in its infancy.

envelope acts as the barrier for the controlled transport of amino acids and other solutes in, and out of, chloroplasts (Weber et al. 2005; Fischer 2011). Numerous highly specific membrane proteins have been identified that mediate the transport of ions and metabolites across the inner envelope membrane (Awai et al. 2006; Facchinelli and Weber 2011; Kunz et al. 2014; López-Millán et al. 2016; Eisenhut et al. 2018; Trentmann et al. 2020), yet plastid amino acid (AA) transporters remain unexplored, with the exception of the CATIONIC AMINO ACID TRANSPORTER PhpCAT from petunia (*Petunia hybrida*) operating in plastidial export of aromatic amino acids in petals (Widhalm et al. 2015). Although not directly functioning in AA transport, it has also been shown that the Arabidopsis (*Arabidopsis thaliana*) DICARBOXYLATE TRANSPORTER DIT2 imports malate into the plastids in exchange with glutamate (Renné et al. 2003).

The principal form of N that is assimilated into organic N is ammonium. It might be taken up directly from the soil or originate from nitrate reduction (Liu and von Wirén 2017; Tegeder and Masclaux-Daubresse 2018). In the final N assimilation step in plastids, ammonium is reduced via the glutamine synthetase/glutamate synthase cycle into glutamine and glutamate. The N from glutamate is then transferred to a variety of carbon precursors, using energy and/or reducing equivalents provided by photosynthesis and subsequently respiration, to produce other amino acids within the plastid (Lawlor 2002; Forde and Lea 2007; Qiu et al. 2020). Asparagine, alanine, and proline are the only proteinogenic amino acids that are generally synthesized in the cytosol, although proline is also produced in chloroplasts under stress (Lam et al. 1998; Székely et al. 2008; Rolland et al. 2012; Alvarez et al. 2022). Based on the locations of de novo AA synthesis, plastidial export of 17 proteinogenic amino acids and import of at least 2 cytosolic amino acids are required for the generation of proteins/enzymes and other N metabolites inside and outside the chloroplasts. However, no chloroplast AA importers or exporters have been characterized in Arabidopsis up to date. Using homology analyses, more than 100 putative Arabidopsis AA transporters were identified but their physiological function in AA transport has only been demonstrated for relatively few proteins, and these are mainly plasma membrane-localized and involved in cellular import (Tegeder and Rentsch 2010; Pratelli and Pilot 2014; Tegeder and Masclaux-Daubresse 2018). Nonetheless, members of the USUALLY MULTIPLE ACIDS MOVE IN AND OUT TRANSPORTER (UMAMIT) family have been shown to facilitate bidirectional transport or cellular efflux of specific amino acids (as well as auxin and glucosinolates) across the plasma membrane or tonoplast (Ladwig et al. 2012; Ranocha et al. 2013; Müller et al. 2015; Besnard et al. 2016, 2018; Zhao et al. 2021; Xu et al. 2023).

In this study, we aimed to discover missing players in AA import into, or export from, Arabidopsis chloroplasts and resolve their physiological function. UMAMIT44 was identified as a potential candidate for plastidial export (see above) since localization prediction programs suggested its targeting of chloroplasts (Supplementary Table S1). Membrane localization was performed with UMAMIT44-green fluorescent protein (GFP) fusion proteins, demonstrating that UMAMIT44 is localized to the chloroplast. Expression studies support the

presence of the transporter in plastids throughout the plant but at higher levels in green tissues. Transport studies in *Xenopus* oocytes, AA profiles, and phenotypic analyses of 2 mutant lines resolved that UMAMIT44 exports glutamate from the chloroplasts and that its function is crucial for plant growth. Physiological, biochemical, and molecular analyses of *umamit44* mutant lines further support that glutamate imbalances inside and outside the plastids affect cellular redox status, result in complex adjustments in plastidial and extraplastidial N and carbon metabolism, and influence the amount of N allocated to growing sinks. Overall, it is concluded that UMAMIT44 function in glutamate export from chloroplasts is essential for regulating N availability for metabolic pathways within source leaf cells as well as for source-to-sink N partitioning and seed yield.

Results

UMAMIT44 is localized to plastids throughout the plant

When screening putative Arabidopsis AA transporters from different gene families (Tegeder and Masclaux-Daubresse 2018) for the presence of chloroplast transit peptides, numerous prediction programs identified UMAMIT44 (At3g28130) as a potential chloroplast/plastid membrane transporter (Supplementary Table S1), including Predotar (Small et al. 2004), WoLF PSORT (Horton et al. 2007), and LOCALIZER (Sperschneider et al. 2017). To resolve the membrane localization *in planta*, UMAMIT44-green fluorescence protein (GFP) fusions were transiently expressed in *Nicotiana benthamiana* protoplasts and leaf cells, respectively. Using chloroplast autofluorescence as control, microscopy imaging showed that UMAMIT44 is indeed localized to the chloroplasts (Fig. 1A). The ring-shaped GFP pattern further suggests UMAMIT44 localization to the chloroplast envelope (c.f. Oikawa et al. 2003; Kunz et al. 2014; Zhang et al. 2018; Yuan et al. 2021). Nevertheless, further work is needed to demonstrate functionality of the localization constructs used in this study.

Expression analysis was performed by reverse transcription polymerase chain reaction (RT-PCR) and RT-qPCR of Arabidopsis plants at the vegetative stage (Fig. 1B). While *UMAMIT44* transcripts were detected throughout the plant, expression was much higher in green tissues (i.e. source and sink leaves) compared to roots pointing, together with the protein localization, to a major role of UMAMIT44 in chloroplast transport processes.

UMAMIT44 function affects levels of specific amino acids and glutathione in chloroplasts and whole leaves

To determine the physiological role of UMAMIT44 *in planta*, 2 homozygous *umamit44* mutant lines with T-DNA insertions in the 3rd intron (*umamit44-1*) and 1st exon (*umamit44-2*) were identified (Fig. 1C). No *UMAMIT44* transcripts were detected in leaves of both mutants (Fig. 1C) indicating a transporter knockout. To resolve if and how UMAMIT44 function in the chloroplast is related to AA transport and if it affects AA homeostasis in the mutants, free AA levels were measured in chloroplasts versus whole leaves (Fig. 2, Supplementary Table S2). While the amounts of total amino acids were unchanged in *umamit44* compared to wild-type (WT) chloroplasts (Fig. 2A), glutamate, glutamine, proline, and alanine levels were significantly increased in both lines (Fig. 2B). At the whole leaf level, total amino acids were reduced in *umamit44* plants (Fig. 2C), which was mainly due to a decrease in glutamate, glutamine, and proline (Fig. 2D, Supplementary Table S2). In addition, leaf amounts of aspartate and lower-abundant leucine and isoleucine were reduced (Supplementary Table S2). Together, these data suggest that, either directly or indirectly, UMAMIT44 plays a role in regulating plastidial and extraplastidial amino acid levels.

We further analyzed the concentrations of the tripeptide glutathione (GSH) which consists of cysteine, glutamate, and glycine and exhibits strong antioxidant properties. Under high oxidative stress, GSH functions as a scavenger for reactive oxygen species (ROS) to reduce the harmful effects of free radicals, and it catalyzes the detoxification of hydrogen peroxide via GSH peroxidase (Noctor et al. 2012; Bela et al. 2015). While levels of reduced GSH (GSH_{red}) were not changed in mutants versus in the wild type, increased amounts of oxidized GSH (GSSG; glutathionedisulfide) were detected in both *umamit44* chloroplasts and whole leaves (Fig. 2, E and F), indicating that the mutant leaves experience oxidative stress, potentially caused by changes in plastidial and/or extra plastidial AA levels (Fig. 2, A to D).

UMAMIT44 is a glutamate exporter, and its function is essential for plant growth

To resolve if the observed accumulation of specific amino acids in *umamit44* chloroplasts (Fig. 2B) is directly linked to UMAMIT44 transport function, efflux studies were performed in *Xenopus* oocytes that expressed *UMAMIT44* cRNA (Fig. 3, A and B). Oocytes, that were initially injected with either *UMAMIT44* cRNA or water (control), were injected with specific radiolabeled amino acids, and oocyte AA levels were measured at injection and after 30 min. No differences in AA levels were found in control oocytes between 0 and 30 min and *UMAMIT44*-expressing oocytes at 0 min (Fig. 3A), indicating functional oocytes without substrate leakage. However, oocytes expressing the transporter showed a significant decrease in labeled glutamate after 30 min compared to the controls, supporting glutamate efflux through UMAMIT44. No differences in AA levels were observed after 30 min between *UMAMIT44*-expressing and control oocytes when labeled glutamine, proline, alanine, or glycine were injected suggesting that these amino acids are not substrates for UMAMIT44 (Fig. 3B). Overall, the

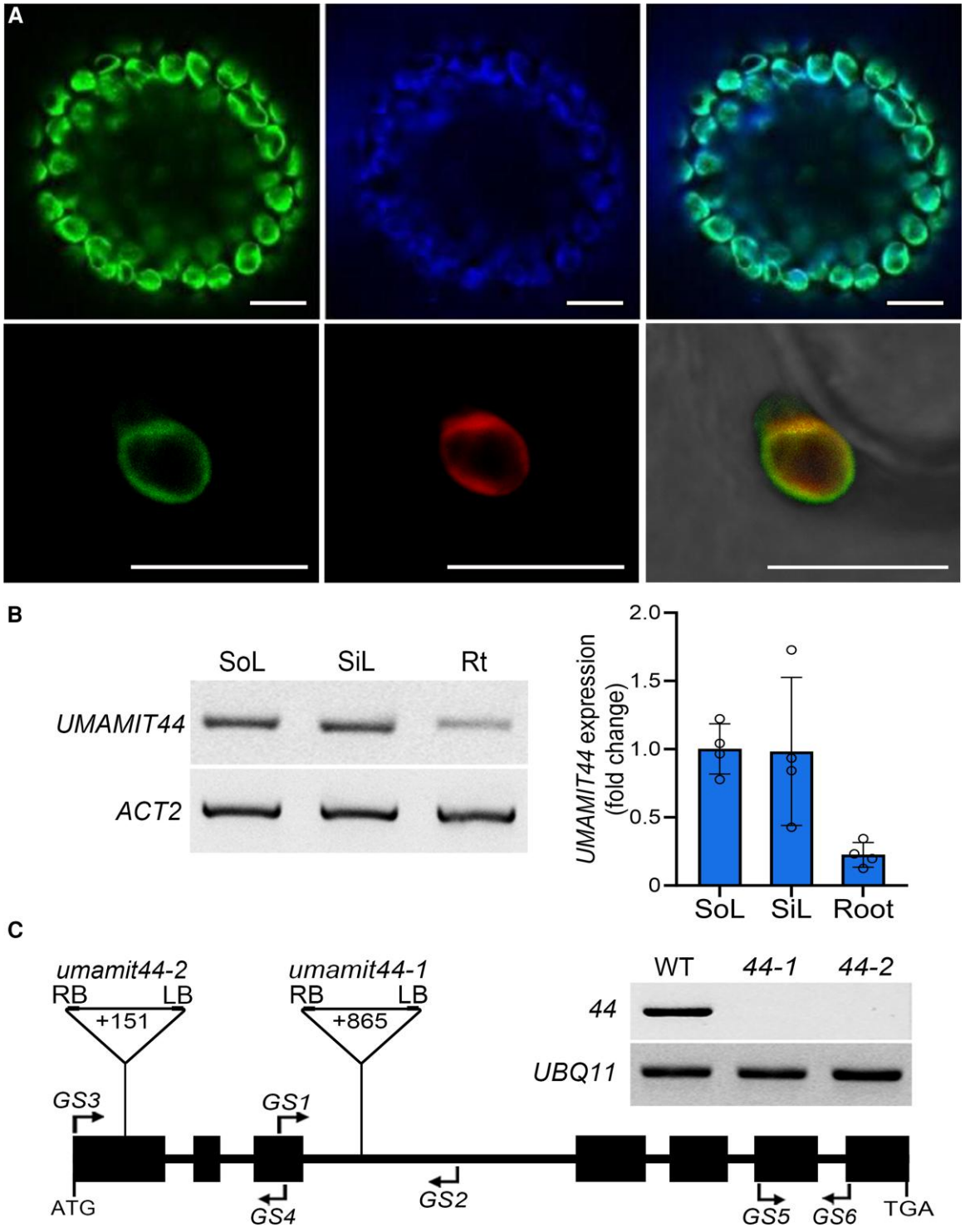

Figure 1. Subcellular localization and organ expression of UMAMIT44. **A)** Subcellular localization of UMAMIT44 in *Nicotiana benthamiana* leaf protoplasts (top images) and leaf cells (bottom). Left images, transient expression of UMAMIT44-GFP fusion proteins. Middle, chloroplast autofluorescence (control). Right, merged images. Results show that both the shorter (At3g28130.1; top) and longer versions (At3g28130.2; bottom) of UMAMIT44 are localized to the chloroplasts. Results were confirmed in at least 2 independent experiments for protoplasts and leaf cells, respectively. Scale bars = 20 μm. **B)** (Left) *UMAMIT44* expression in source (SoL) and sink leaves (SiL), and roots (Rt) of 4-wk-old WT Arabidopsis plants using RT-PCR. *ACTIN2* (*ACT2*) was used as control for equal amounts of RNA. (Right) RT-qPCR analysis of *UMAMIT44* expression ($n = 4$). **C)** *UMAMIT44* expression analysis in *umamit44-1* and *umamit44-2* mutant lines. (Left) Positions of T-DNA insertions in the 2 mutants. Boxes and lines represent exon and intron regions, respectively. Inverted triangles indicate the locations of T-DNA insertions (+865 nucleotides downstream of the start codon/ATG in *umamit44-1* and +151 nucleotides for *umamit44-2*). Corner arrows indicate primer positions: GS1 to GS4 primers were used for mutant screening, and GS5 and GS6 for RT-PCR. (Right) *UMAMIT44* expression in mutant and WT source leaves using RT-PCR. *UBIQUITIN11 (UBQ11)* was amplified as an internal control for equal amounts of RNA. Error bars depict ± SD. See Supplementary Table S3 for primer information.

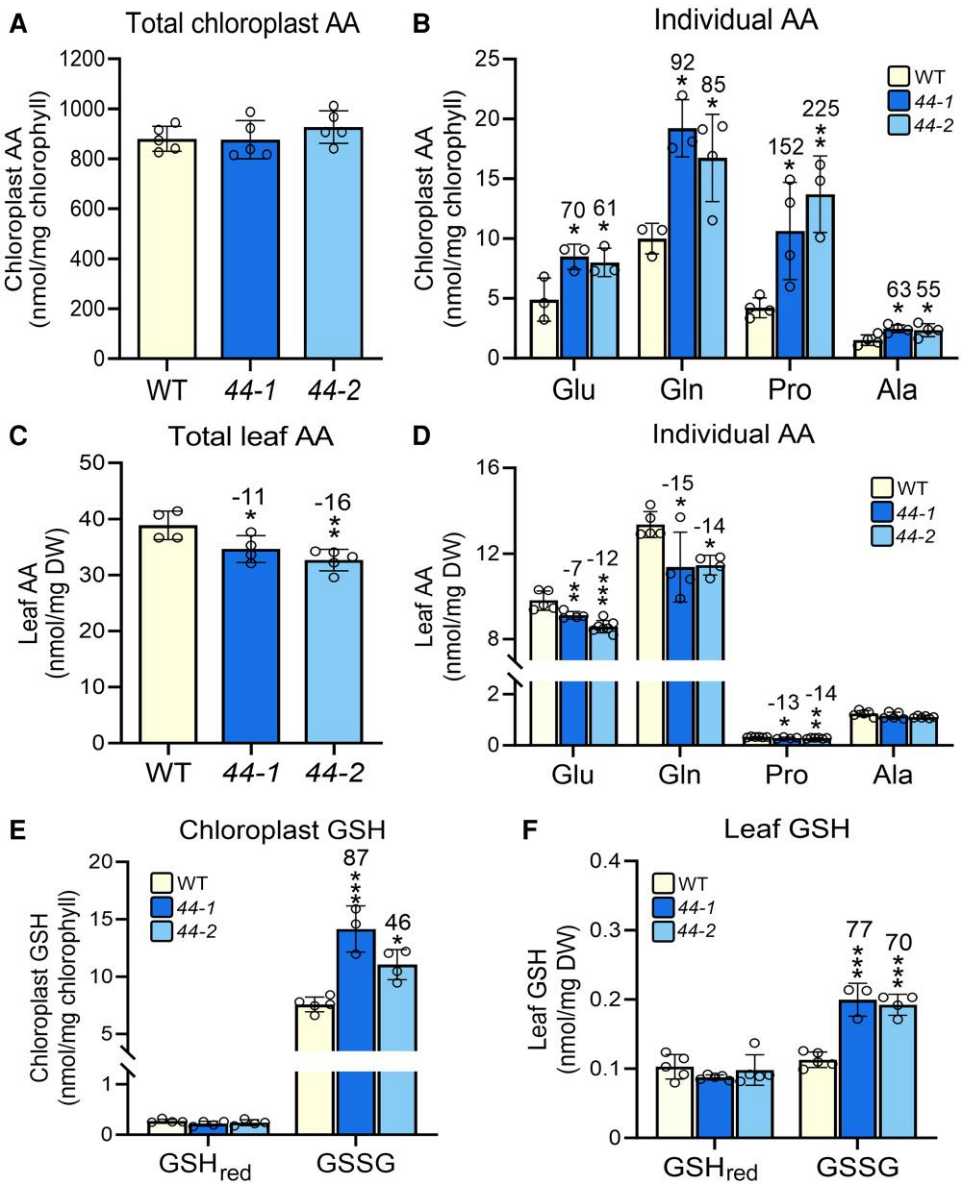

Figure 2. Analysis of AA and GSH concentrations in chloroplasts and whole leaves of *umamit44* and WT plants. **A)** Total free AA content in chloroplasts ($n = 5$). **B)** Chloroplast glutamate (Glu), glutamine (Gln), proline (Pro), and alanine (Ala) levels ($n = 3$ to 4). **C)** Total free AA content in leaves ($n = 4$ to 5). **D)** Leaf Glu, Gln, Pro, and Ala levels ($n = 4$ to 7). **E and F)** Reduced (GSH_{red}) and oxidized (GSSG) GSH in (E) chloroplasts ($n = 3$ to 5; note the y-axis break) and (F) leaves ($n = 3$ to 5). Data points superimposed over the bar graphs represent an individual plant. Error bars depict ± SD, asterisks indicate levels of significant differences from WT (*$P < 0.05$; **$P < 0.01$; ***$P < 0.001$), and numbers above the columns describe the percentage change in *umamit44* versus WT. DW, dry weight.

transport studies (Fig. 3, A and B) together with the subcellular localization (Fig. 1A), expression analyses (Fig. 1, B and C) and the accumulation of glutamate in the mutant chloroplasts (Fig. 2B) support that UMAMIT44 exports glutamate from green plastids.

Phenotypic analyses were performed to determine the importance of UMAMIT44 function in plastidial glutamate export for plant growth. Results showed a significant decrease in leaf surface area and a reduction in shoot biomass in the *umamit44* lines (Fig. 3, C and D).

The lack of UMAMIT44 function in glutamate efflux leads to a rebalancing of n metabolism inside and outside the chloroplasts

Glutamine, proline, and alanine are not exported from oocytes by UMAMIT44 (Fig. 3B) but accumulate in mutant chloroplasts besides glutamate (Fig. 2B). Since some of the piled-up glutamate may be channeled into plastidial glutamine or proline synthesis, expression analysis of respective synthesis genes, that have been reported to be transcriptionally regulated, was performed. Results showed an upregulation of

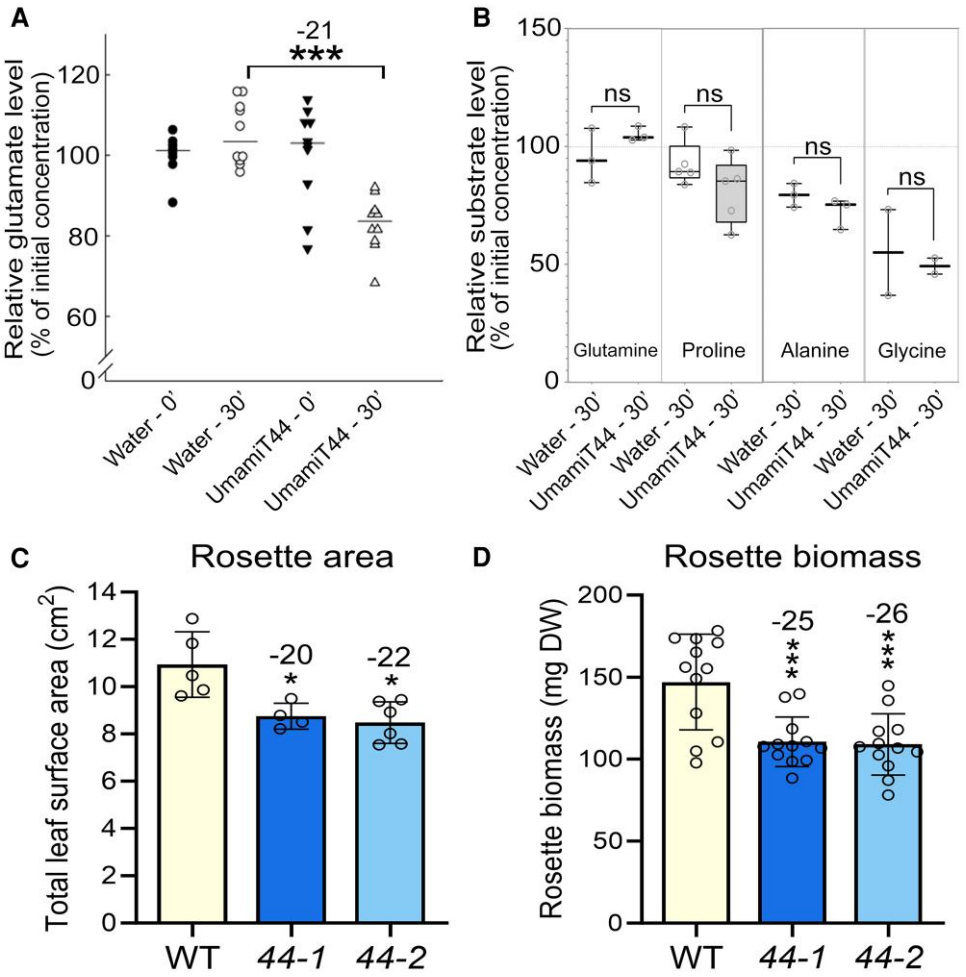

Figure 3. Transport studies in *Xenopus* oocytes and growth analysis of *umamit44* mutant plants. **A and B)** Efflux of amino acids from oocytes expressing UMAMIT44. Oocytes were injected with either *UMAMIT44* cRNA or water (control) 4 d before the injection with 5 mM of radiolabeled (A) glutamate, (B) glutamine, proline, alanine, and glycine ($n = 10$). Levels of amino acids in oocytes were measured immediately after injection (0′) and after 30 min (30″). Error bars depict ± SD, asterisks show levels of significant differences from WT (***$P < 0.001$), and n.s. indicates statistically non-significant differences. The number above the bracket describes the percentage change in glutamate levels in oocytes injected with water versus *UMAMIT44* cRNA. **C)** Rosette leaf area ($n = 4$ to 6) and **D)** rosette biomass (DW, dry weight; $n = 12$) of 4-wk-old mutant and WT plants. Data points superimposed over the bar graphs represent individual plants. Error bars depict ± SD, asterisks indicate levels of significant differences from WT (*$P < 0.05$; **$P < 0.01$; ***$P < 0.001$), and numbers above the columns describe the percentage change in *umamit44* versus WT.

GLUTAMINE SYNTHETASE 2 (*GLN2*) and no change in *GLUTAMATE SYNTHASE 1* (*GLU1*) and *GLU2* transcript levels in *umamit44 versus* WT leaves (Fig. 4A). Further, expression of *PYRROLINE-5-CARBOXYLATE SYNTHASE 1* (*P5CS1*) encoding for the plastidic/cytosolic pyrroline-5-carboxylate synthase essential for proline synthesis was significantly increased. Although de novo synthesis of alanine occurs in the cytosol, in plastids it may be produced from cysteine involving *NIFS-LIKE CYSTEINE DESULFURASE 2* (*NFS2*), a cysteine desulfurase gene, but its expression was not changed (Fig. 4B). In line with the observed high amounts of total GSH (Fig. 2E), transcript levels of *γ-GLUTAMYLCYSTEINE SYNTHETASE 1* (*GSH1*) were upregulated (Fig. 4B).

Decreased export of glutamate from *umamit44* plastids and its reduced availability in the mutant cytosol (Fig. 2, B and D; Supplementary Table S2) may, to some extent, be counterbalanced by other yet unknown glutamate efflux systems or by DiT2, a dicarboxylate transporter that imports malate in exchange with glutamate (Renné et al. 2003). However, DiT2 expression was not altered (Fig. 4C). Alternatively, increased chloroplast export of glutamine or other amino acids such as phenylalanine may occur which can then be used for extra plastidial glutamate production. A potential candidate facilitating this step is Arabidopsis CATIONIC AMINO ACID TRANSPORTER 7 (CAT7), the closest homolog to petunia PhpCAT plastidial exporter for phenylalanine and other aromatic amino acids (Widhalm et al. 2015). Transcript levels of *CAT7* were upregulated in *umamit44* leaves (Fig. 4C).

It is generally assumed that subcellular AA levels may be monitored by sensors triggering complex signaling cascades and adjustments in metabolic pathways, but the underlying

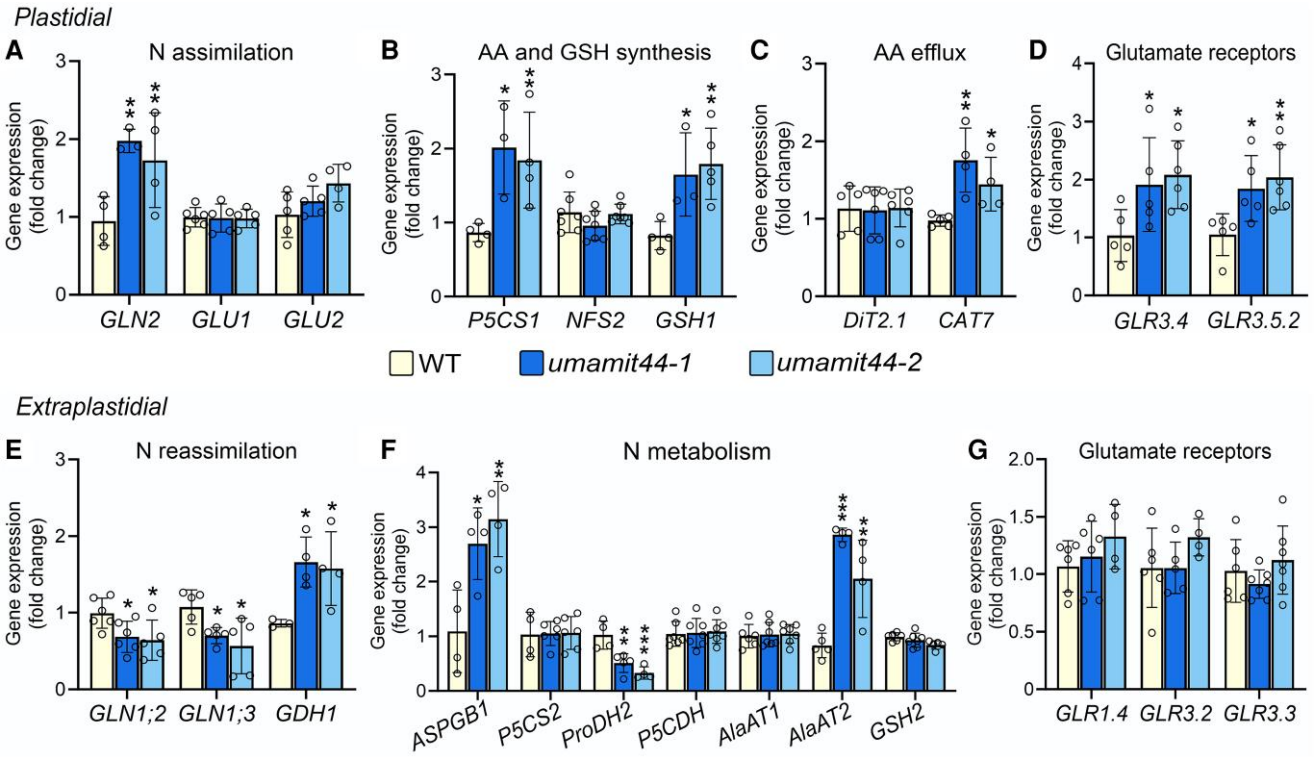

Figure 4. Expression analysis of genes involved in plastidial and extraplastidial nitrogen (N) metabolism, transport and signaling. **A to D)** Leaf expression of genes encoding products involved in plastidic (A) N assimilation (*GLN2*; *GLUTAMATE SYNTHASE GLU1*, and *GLU2*), **B)** synthesis of the amino acids (AA) proline and alanine, and GSH synthesis (*P5CS1*, *PYRROLINE-5-CARBOXYLATE (P5C) SYNTHETASE 1*; *NFS2*, *NIFS-LIKE CYSTEINE DESULFURASE 2* involved in removal of sulfur from cysteine to produce L-alanine; *GSH1*, *γ-GLUTAMYLCYSTEINE SYNTHETASE 1*), **C)** AA efflux (*DiT2.1*, *DICARBOXYLATE TRANSPORTER 2.1*; *CAT7*, *CATIONIC AMINO ACID TRANSPORTER 7*), and **D)** glutamate signaling through inner envelope-localized *GLR*s channels *GLR3.4* and *GLR3.5.2*. **E to G)** Expression of genes encoding products involved in extraplastidial (E) N re-assimilation (*GLUTAMINE SYNTHETASE GLN1; 2* and *GLN1; 3*; *GDH1*, *GLUTAMATE DEHYDROGENASE 1*), (F) proline, alanine, and GSH synthesis (*P5CS2*, *PYRROLINE-5-CARBOXYLATE (P5C) SYNTHETASE 2*; *ALANINE AMINOTRANSFERASE AlaAT1* and *AlaAT2*; *GSH2*, *γ-GLUTAMYLCYSTEINE SYNTHETASE 2*), and asparagine and proline catabolism (*ASPARAGINASE B1*, *ASPGB1*; *ProDH2*, *PROLINE DEHYDROGENASE 2*; *P5CDH*, *P5C DEHYDROGENASE*), and (G) glutamate signaling through plasma membrane-localized GLRs (*GLR1.4*, *GLR3.2*, *GLR3.3*). For primer information see Supplementary Table S3. ($n = 3$ to 7). Data points superimposed over the bar graphs represent individual plants. Error bars depict ± SD; asterisks indicate levels of significant differences from WT (*$P < 0.05$; **$P < 0.01$; ***$P < 0.001$).

mechanisms remain elusive. Yet, recent work suggests a role of membrane-localized glutamate receptor-like (GLR) channels in glutamate signaling (Simon et al. 2023), and expression analysis revealed significant increases in plastidial *GLR3.4* and *GLR3.5.2* transcript levels in *umamit44* leaves (Fig. 4D).

Enhanced catabolism or deamination reactions of amino acids, or decreased glutamine synthesis outside the *umamit44* plastids may serve as a compensatory mechanism to mitigate the deficit of cytosolic glutamate. Results showed that *GLN1; 2* and *GLN1; 3*, encoding products important for cytosolic N re-assimilation, were downregulated, and expression of *glutamate dehydrogenase 1* (*GDH1*), encoding a product implicated in the reversible conversion of glutamate to 2-oxoglutarate and ammonia outside the plastids, was upregulated in *umamit44* leaves (Fig. 4E). Further, transcript levels of *ASPGB1*, encoding a product important for deamination of asparagine and the release of ammonium for re-assimilation, were increased (Fig. 4F). No change in mutant leaf expression was observed for the cytosolic proline synthesis gene *P5CS2*, while unchanged and decreased transcript levels were detected for *P5CDH* or *ProDH2*, which encode products involved in converting proline to glutamate (Fig. 4F). Expression of genes encoding extraplastidial alanine aminotransferases, functioning in the reversible conversion of pyruvate and glutamate to alanine and 2-oxoglutarate, were either not changed (*AlaAT1*) or upregulated (*AlaAT2*) in mutant leaves compared to in WT leaves (Fig. 4F), and no changes were observed for *GSH2*, encoding a product involved in cytosolic GSH synthesis or for plasma membrane receptor genes *GLR1.4*, *GLR3.2*, and *GLR3.3* (Fig. 4, F and G).

The *umamit44* growth phenotype can be recovered by feeding specific amino acids

Mutant and WT plants were grown on media supplied with individual amino acids to analyze if the *umamit44* growth phenotype can be complemented by exogenous application

of glutamate or amino acids that are generally found in relatively high concentrations in leaf cells and can be used to generate glutamate outside the plastids (Fig. 5). Like for soil-grown plants (Fig. 3D), results showed a significant reduction in shoot biomass of 21% to 28% for the mutant lines grown on control medium (Fig. 5). When fed with glutamate, glutamine, or proline, similar biomass was obtained for *umamit44* and WT plants, demonstrating that external supply of these amino acids fully restores mutant growth to WT level. No effect on mutant growth was found for aspartate and alanine, while some growth recovery was observed for asparagine as indicated by only a 9% to 11% decrease in *umamit44* shoot biomass.

Carbon metabolism is altered in *umamit44* mutants

We further examined if and how UMAMIT44 function in chloroplasts affects interconnected carbon (C) metabolism (Fig. 6, A to I). First, gas exchange measurements were performed, and results showed that photosynthetic rates were significantly decreased in the *umamit44* mutant lines (Fig. 6A). Absorbed light energy is mainly used to drive photochemistry, but some excitation energy is dissipated as heat in nonphotochemical quenching (NPQ) or emitted as fluorescence radiation to protect against adverse effects of high light intensity. No differences were observed for F_v/F_m (variable versus maximum chlorophyll a fluorescence yield) between *umamit44* and WT plants (Fig. 6B), and NPQ was generally not changed (Fig. 6C). When analyzing the actual quantum efficiency of electron flux through PSII (Φ_{PSII}) it was generally lower in the mutants (Fig. 6D). Together with the gas exchange experiments (Fig. 6A), this suggests an effect on PSII photochemistry in *umamit44* plants resulting in decreased efficiency of photochemical reactions and ultimately reduced leaf C fixation.

Analysis of fixed leaf C pools showed no change for sucrose (Fig. 6E) but a decrease in glucose levels in *umamit44* leaves (Fig. 6F). Besides directed C allocation toward sucrose and glucose, relatively large amounts of photosynthetically fixed C is channeled toward the shikimate pathway to produce aromatic amino acids including phenylalanine (Schenck and Maeda 2018; Lynch and Dudareva 2020) and downstream derivatives such as anthocyanin and other flavonoids that act as free radical scavengers against ROS (Heim et al. 2002; Das and Roychoudhury 2014; Kovinich et al. 2015). Levels of anthocyanin and other flavonoids were significantly higher in *umamit44* leaves compared to in WT leaves (Fig. 6, G and H). In addition, expression of *CHALCONE SYNTHASE* (*CHS*), which encodes for the first committed enzyme and rate-limiting step in flavonoid biosynthesis (Feinbaum and Ausubel 1988; Grotewold 2006; Saito et al. 2013), as well as *FLAVONOL SYNTHASE 3* (*FLS3*), encoding a product involved in downstream formation of flavonols (Preuß et al. 2009), were upregulated (Fig. 6I). Levels of hydrogen peroxide (H_2O_2), a major ROS that accumulates under stress, showed no changes in *umamit44* plants (Fig. 6J). Together the results suggest that *umamit44* leaves experience oxidative stress and use flavonoids as a protection mechanism (Fig. 6, G to J). Flavonoid synthesis from phenylalanine also results in the release of ammonium that can be used for N re-assimilation into glutamate (see Fig. 8).

UMAMIT44 function affects source-to-sink transport of N and C, and sink development

It was further examined if decreased export of glutamate from *umamit44* chloroplasts and, consequently, reduced cytosolic levels of major amino acids (see Fig. 2, A to D; Supplementary Table S2) affect source-to-sink transport of amino acids via the phloem (Fig. 7, A to C). First, expression of transporter genes involved in leaf phloem loading of amino acids was analyzed, and results resolved significantly reduced transcript levels for *AMINO ACID PERMEASE 8* (*AAP8*) and *CAT6* in *umamit44* leaves (Fig. 7A), suggesting decreased AA export from leaves and long-distance transport in the phloem. This was further examined by leaf phloem exudate analyses demonstrating a decrease in total AA levels in *umamit44* exudates, which was mostly due to reduced glutamate, glutamine, proline, alanine, and asparagine levels (Fig. 7, B and C; Supplementary Table S2). In addition, sucrose levels in phloem exudates of *umamit44* leaves were significantly reduced (Fig. 7D). Together, the changes in N and C allocation to sinks resulted in significantly decreased seed yields of 21% and 24%, dependent on the *umamit44* line (Fig. 7E), and a reduction in seed protein content by up to 25% (Fig. 7F).

Discussion

Amino acids are fundamental components of complex plant metabolic networks involving numerous cellular compartments. As plastids are the location of N assimilation and de novo biosynthesis of most proteinogenic amino acids, membrane transporters are required to regulate their export from the stroma to the cytosol to accommodate numerous subcellular biochemical pathways, as well as the N demand of sinks (The et al. 2021). In the current study, an Arabidopsis plastidial AA transporter, called UMAMIT44, was identified (Fig. 1). UMAMIT44 localization (Fig. 1A) and transport studies (Fig. 3, A and B) as well as *umamit44* mutant analyses showing accumulation of glutamate in *umamit44* chloroplasts (Fig. 2B) and decreased glutamate amounts at whole leaf level (Fig. 2D) support that UMAMIT44 transports glutamate from the chloroplasts to the cytosol via the plastidial envelope. Since the chloroplast outer envelope is not selective for AA movement (Pohlmeyer et al. 1997; Steinkamp et al. 2000), it is reasonable to assume that UMAMIT44 regulates glutamate efflux across the inner envelope membrane. Additionally, our data demonstrate that UMAMIT44 is an essential transporter, since reduced plastidial export of glutamate and its limited availability for extraplastidial metabolic pathways (Fig. 2, C and D) and for source-to sink transport (Fig. 7, B and C) result in strongly reduced

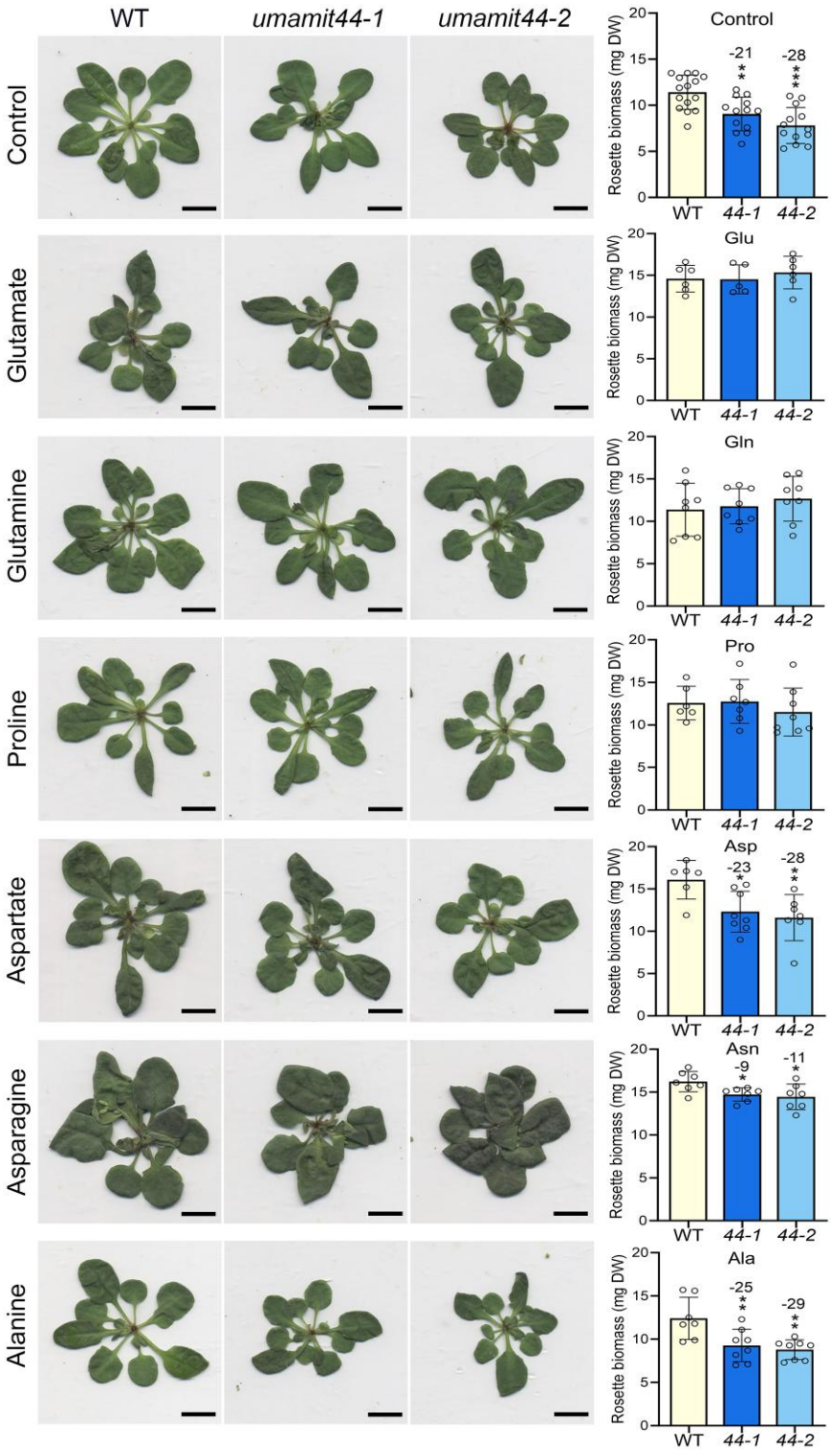

Figure 5. Growth phenotype and shoot biomass of *umamit44* plants cultured on media supplemented with specific amino acids. WT plants and *umamit44-1* (*44-1*) and *umamit44-2* (*44-2*) lines were grown on normal MS medium (control) or on MS media supplemented with glutamate (50 mM Glu), glutamine (25 mM Gln), proline (25 mM Pro), aspartate (10 mM Asp), asparagine (10 mM Asn), or alanine (25 mM Ala). Plants were harvested after 14 d of growth, pressed between two layers of transparent foil, imaged using a flatbed scanner, and then used for rosette biomass analysis (DW, dry weight) ($n = 8$ to 15). Data points superimposed over the bar graphs represent individual plants. Error bars depict ± SD, asterisks indicate levels of significant differences from WT (*$P < 0.05$; **$P < 0.01$; ***$P < 0.001$), and numbers above the columns describe the percentage change in *umamit44* versus WT. Scale bars = 1 cm.

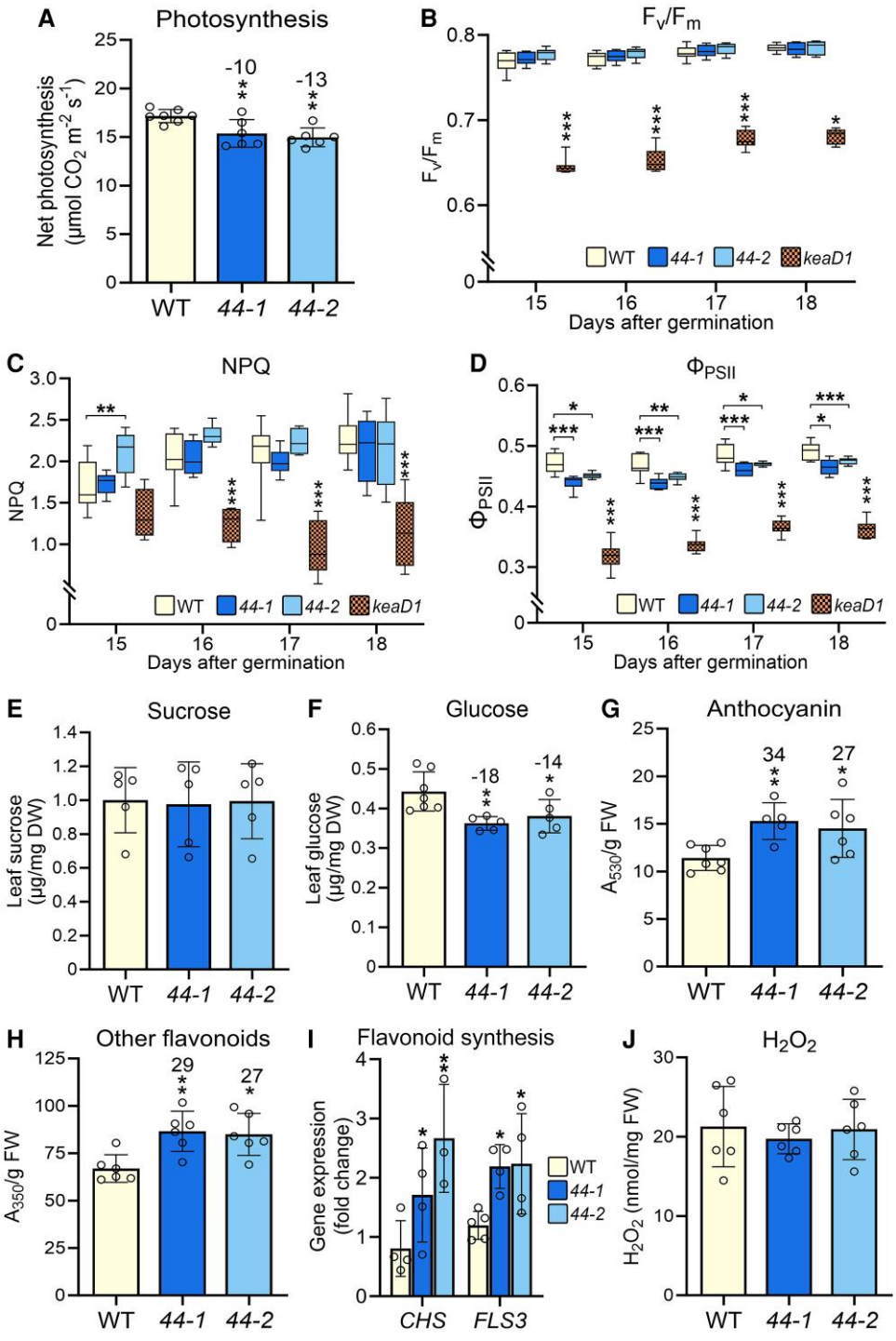

Figure 6. Analyses of photosynthetic parameters, carbon metabolites and other factors related to oxidative stress. **A)** Leaf photosynthetic rate ($n = 6$ to 7). **B-D)** Analyses of chlorophyll fluorescence parameters in *umamit44* lines, WT (control) and *keaD1* plants (control; double mutant line of inner-envelope K^+ efflux antiporters *KEA1* and *KEA2*, Kunz et al. 2014). Results are shown as box plots, with the line within each box representing the median and the minimum and maximum values being indicated at the end of the lower and upper whiskers, respectively ($n = 6$ to 12). **B)** Maximum quantum efficiency of photosystem (PS) II (F_v/F_m). **C)** NPQ. **D)** Photochemical efficiency of PSII (Φ_{PSII}). **E)** Leaf sucrose levels ($n = 5$). **F)** Leaf glucose levels ($n = 5$ to 7). **G)** Leaf anthocyanin ($n = 5$ to 7) and **(H)** other flavonoids ($n = 6$). **I)** Expression analysis of genes encoding products involved in flavonoid biosynthesis ($n = 3$ to 5). **J)** Hydrogen peroxide (H_2O_2) ($n = 6$). Data points superimposed over the bar graphs represent individual plants. Error bars depict ± SD, asterisks indicate levels of significant differences from WT (*$P < 0.05$; **$P < 0.01$; ***$P < 0.001$), and numbers above the columns describe the percentage change in *umamit44* versus WT.

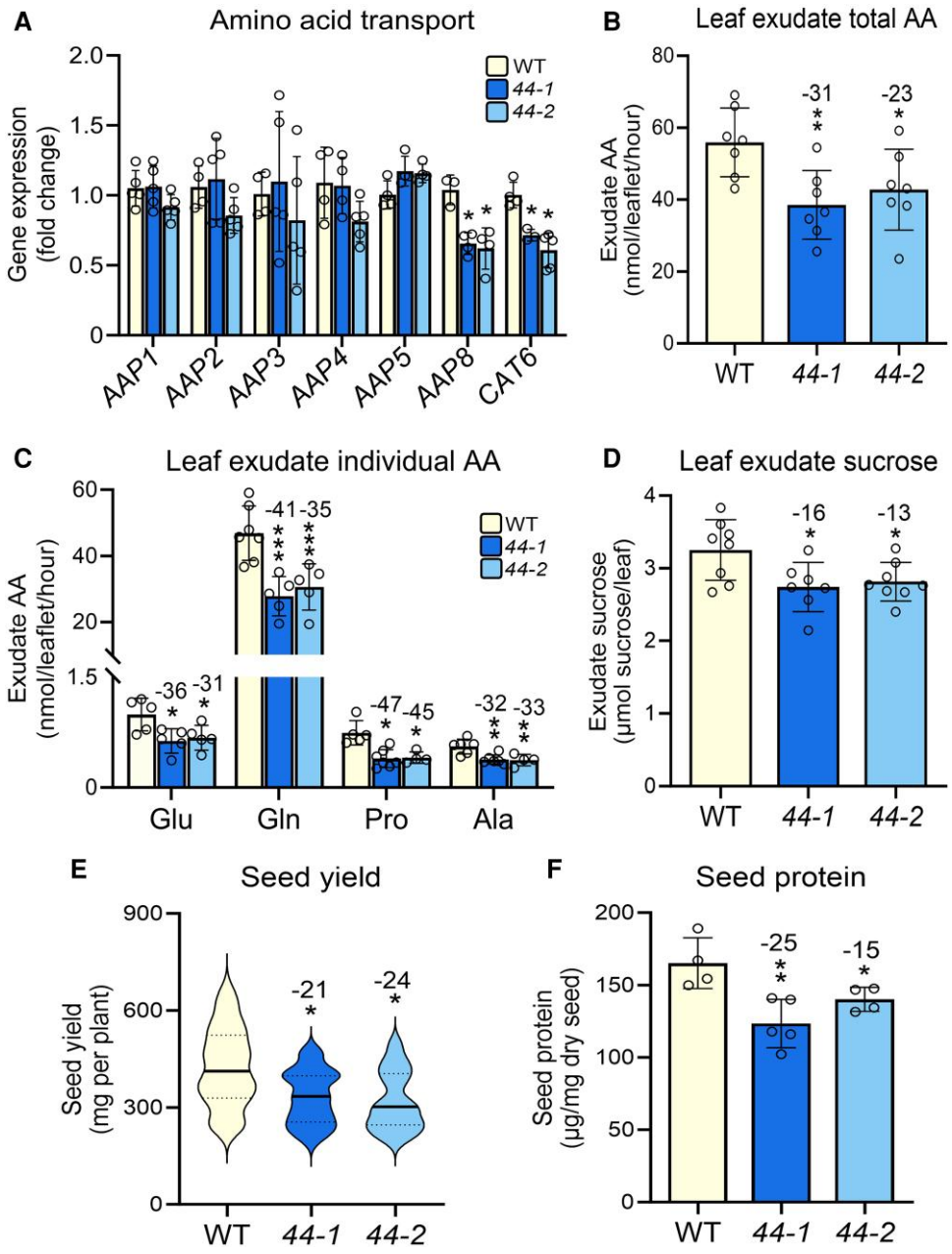

Figure 7. Analysis of source-sink transport of nitrogen and carbon, seed yield and seed protein levels. **A)** Expression analysis of plasma membrane-localized AA phloem loaders using RT-qPCR ($n = 3$ to 5). See Supplementary Table S3 for primer information. **B to D)** Analysis of leaf exudates. **B)** Total free AA ($n = 7$). **C)** Individual AA ($n = 4$ to 7). **D)** Sucrose ($n = 7$ to 8). **E)** Seed yield ($n \geq 37$). Results are shown as violin plots, with the bold line in the plot representing the median, and the lower and upper dashed lines the first and third quartile, respectively. **F)** Total soluble protein in dry seeds ($n = 4$ to 5). Data points superimposed over the bar graphs represent individual plants. Error bars depict ± SD, asterisks indicate levels of significant differences from WT (*$P < 0.05$; **$P < 0.01$; ***$P < 0.001$), and numbers above the columns describe the percentage change in *umamit44* versus WT.

vegetative growth of *umamit44* lines (Fig. 3, C and D). The growth phenotype can be recovered by externally supplied glutamate (Fig. 5) further supporting the shortage of cytosolic glutamate in the mutants for downstream physiological processes and that UMAMIT44 is a key player in maintaining glutamate homeostasis.

Nevertheless, since the knockout in *UMAMIT44* is not lethal, other transporters may move some glutamate to the cytosol (Renné et al. 2003; Figs. 4C and 8). Additionally, *umamit44* plants may compensate, at least to some extent, for the loss of UMAMIT44 function in glutamate export by generating increased amounts of amino acids that can be used for glutamate production outside the chloroplasts, such as glutamine, proline, and alanine (c.f. Hildebrandt et al. 2015 and within). Glutamine restores *umamit44* growth to normal when fed to the mutants (Fig. 5) and seems to be the major

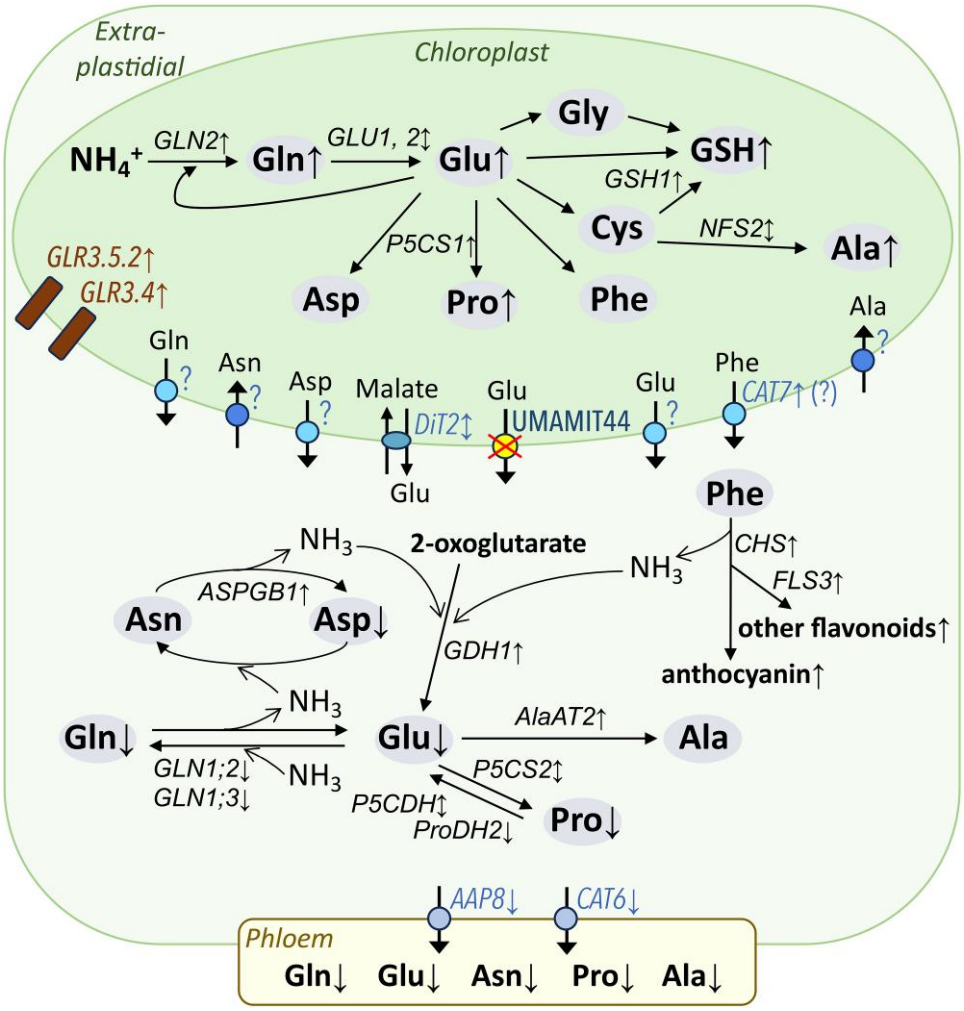

Figure 8. Model of plastidial and extraplastidial nitrogen metabolism and transport processes in leaves of *umamit44* lines. The loss of UMAMIT44 function in glutamate (Glu) export from chloroplasts causes accumulation of Glu in plastids and subsequently its decreased availability outside the plastids/at whole leaf level. While some Glu may still be moved out of chloroplasts via DiT2 or by a yet unknown Glu efflux system, the Glu imbalance results in numerous adjustments to ensure continuation of *umamit44* chloroplast function, cellular metabolism, nitrogen (N) allocation, and source-to-sink transport of amino acids. Within the chloroplasts, N assimilation continues, and Glu is channeled into increased glutamine (Gln) synthesis as well as higher production of proline (Pro) and GSH, the latter 2 mitigating oxidative damage. On the other hand, increased plastid levels of alanine (Ala) seem to originate from its increased extraplastidial synthesis and chloroplast import. No changes in phenylalanine (Phe) levels in chloroplasts and whole leaves of mutants, increased expression of the putative Phe exporter gene *CAT7* and higher extraplastidial flavonoid synthesis support that Glu is also used to produce more Phe for increased production of flavonoids, additionally functioning in oxidative stress response. Changes in cytosolic Glu or the N status and signaling may involve Glu receptor-like (GLR) ion channels leading to the observed adjustments in N (and C) metabolism and transport. The decreased availability of Glu for physiological processes outside the chloroplasts is alleviated by (i) decreased Glu usage for cytosolic N re-assimilation and Gln synthesis through glutamine synthetase1 (encoded by *GLN1; 2* and *GLN1; 3*), as well as for proline synthesis and (ii) increased N re-assimilation and direct Glu production via Glu dehydrogenase GDH1. Ammonia (NH_3) for re-assimilation may originate from multiple sources including from Phe used for flavonoid synthesis as well as Gln. Higher amounts of plastid Gln are exported by an unknown transporter and used for cytosolic Glu production, most likely via asparagine (Asn) and its deamination. The lack of UMAMIT44-mediated Glu export from chloroplasts not only results in a complex rebalancing of source N (and C) metabolism, but also affects phloem loading of amino acids and sink N supply. Arrows with circles indicate transporters and "X" refers to knockout of *UMAMIT44*. Upward arrows indicate upregulation or increases, downward arrows downregulation or decreases, and double-headed arrows no change. Question marks refer to yet unknown transporters. NH_4^+, ammonium; Asp, aspartate; Cys, cysteine; Gly, glycine. For specific genes see Supplementary Table S3.

player in warranting glutamate availability in the *umamit44* cytosol via 2 strategies. First, higher amounts of glutamine are produced in the *umamit44* chloroplasts, exported, and used for cytosolic glutamate production, most likely via asparagine which also partially recovers the growth phenotype of *umamit44* plants (Figs. 5 and 8). This prediction is in agreement with the (i) upregulation of the plastidial *GLN2* (Fig. 4A), (ii) increased glutamine chloroplast levels (Fig. 2B) and (iii) decreased whole leaf and phloem glutamine levels (Figs. 2, D and 7C), as well as with (iv) decreased leaf

aspartate amounts (Supplementary Table S2), (v) upregulation of expression of *ASPGB1* associated with deamination of asparagine (Fig. 4F), and (vi) reduced levels of asparagine in leaf phloem exudates (Supplementary Table S2). Second, re-assimilation of ammonium released from asparagine and other metabolic pathways generally occurs through cytosolic glutamine synthetases using glutamate as a substrate (c.f. Xu et al. 2012; Hildebrandt et al. 2015; Fig. 8). However, in *umamit44* leaves, *GLN1* genes were downregulated while *GDH1* was significantly upregulated suggesting (i) that cytosolic glutamine synthesis is decreased to preserve glutamate availability for other essential physiological processes and (ii) that some re-assimilation occurs via glutamate dehydrogenase to directly produce additional glutamate for cellular metabolism (Fig. 8; Masclaux-Daubresse et al. 2010; Gaufichon et al. 2016 and ref within). Increased amounts of ammonium for N re-assimilation into glutamate also derive from deamination of phenylalanine that is used toward enhanced flavonoid synthesis in *umamit44* leaves (Figs. 6, G to I, and 8). Future experiments will need to address if adjustments in other catabolic pathways also participate in metabolic plasticity and formation of glutamate outside of the *umamit44* chloroplasts and to identify further interconnected metabolic processes, for example by using transcriptomics (Krouk et al. 2010; Contreras-López et al. 2022; Durand et al. 2023; Wang et al. 2023), and crucial $^{13}CO_2$ labeling (Arrivault et al. 2017; Treves et al. 2022; Xu et al. 2022) and metabolic flux analyses (Allen et al. 2009; Ma et al. 2014; Hildebrandt et al. 2015; Lynch and Dudareva 2020). At least alanine does not provide a main route for alternative glutamate production as it is unable to recover the *umamit44* growth phenotype (Fig. 5). *De novo* biosynthesis of alanine takes place outside the plastids, and upregulated expression of extraplastidial *AlaAT2* (Fig. 4F), reduced alanine amounts in phloem exudates (Fig. 7C), but increased levels in mutant chloroplasts (Fig. 2B) rather suggest enhanced alanine synthesis and import into *umamit44* chloroplasts by an unknown transport mechanism (Fig. 8) to potentially attenuate stress triggered by buildup of glutamate (Sato et al. 2002; Ricoult et al. 2005; Miyashita et al. 2007; Limami et al. 2008). Moreover, cytosolic proline synthesis and its usage for glutamate production appear to be not changed or downregulated as no changes or decreases were observed in expression for extraplastidial proline synthesis and catabolism genes (Fig. 4F) and both whole leaf and phloem proline levels were declined in the mutants (Figs. 2, D and 7C). On the other hand, upregulation was found for plastidic/cytosolic *P5CS1* (Fig. 4B) which is most probably responsible for proline synthesis in *umamit44* chloroplasts as supported by high plastidial proline levels (Fig. 2B). Similarly, upregulation of *P5CS1*, accumulation of plastidial P5CS1-GFP proteins and increases in proline pools have been reported for Arabidopsis plants exposed to abiotic stress (Yoshiba et al. 1995; Strizhov et al. 1997; Székely et al. 2008). In *umamit44* chloroplasts, the increased synthesis of proline from glutamate and proline accumulation may have a 2-fold benefit: the reduction of otherwise damaging high glutamate pools, and the production of a multifunctional AA with diverse roles in alleviating plastidial stress (Hong et al. 2000; Matysik et al. 2002; Kishor et al. 2005; Szabados and Savouré 2010). The lower quantum efficiency of PSII and significantly reduced photosynthesis rates in *umamit44* leaves (Fig. 6, A and D) demonstrate some adverse effects on photosynthetic energy transfer and C fixation. Increased proline synthesis and associated generation of $NAD^+/NADP^+$ electron carriers may be required in *umamit44* plastids to stabilize cellular redox balance and prevent damage to the photosynthetic apparatus (Hare and Cress 1997; Sharma et al. 2011; Hashida et al. 2018).

ROS form as by-products of electron transport chains or redox reactions in chloroplasts (and other compartments) and lead to oxidative stress (Mittler et al. 2004; D'Autréaux and Toledano 2007; Hossain et al. 2015). Depending on the concentration, ROS can be damaging to cellular components (Halliwell 2006; Petrov et al. 2015; Qi et al. 2018), but at proper levels, they act as signaling compounds for plant developmental processes and stress responses (Baxter et al. 2014; Mittler et al. 2022). This intricate function implies that the rates of ROS generation and degradation must be controlled at subcellular and cellular levels (Meyer et al. 2012; Müller-Schüssele et al. 2020). One strategy to adjust ROS levels and reduce oxidative damage is the production of antioxidants. In *umamit44* chloroplasts, excess glutamate may lead to changes in the steady-state levels of ROS triggering the synthesis of ROS scavengers (Mittler et al. 2022). This is not only in line with the significant increase in proline (Fig. 2B), that stabilizes antioxidant enzymes and potentially serves direct antioxidant function (Alia et al. 2001; Matysik et al. 2002; Alvarez et al. 2022), but also with a substantial increase in oxidized GSH at both the *umamit44* plastid and whole leaf level (Fig. 2, E and F; Noctor and Foyer 1998; Pfannschmidt 2003). Further, levels of anthocyanins and other flavonoids were strongly elevated (Fig. 6, G to I), most probably additionally diminishing glutamate-induced oxidative damage in the mutant leaves (Hahlbrock and Scheel 1989; Mehrtens et al. 2005; Preuß et al. 2009; Zhang et al. 2017). Overall, the observed adjustments in oxidative stress response and antioxidant production (i.e. more proline, GSH, and flavonoids) seem to be effective as no differences were found in H_2O_2 levels in *umamit44* leaves compared to in WT leaves (Fig. 6J).

Flavonoids are mainly produced in the cytosol, and the biosynthesis pathways heavily rely on phenylalanine biosynthesis and its subsequent export out of plastids (Maeda and Dudareva 2012), which is mediated in petunia by PhpCAT (Widhalm et al. 2015). *CAT7*, which is the closest Arabidopsis homolog and encodes a putative plastid transporter (Su et al. 2004), was upregulated in *umamit44* leaves and may facilitate enhanced movement of the aromatic AA from the plastids to the cytosol. Interestingly, phenylalanine synthesis and downstream flavonoid production and accumulation are also increased by N stress (Stewart et al. 2001;

Lea et al. 2007; Lillo et al. 2008; Peng et al. 2008; Rubin et al. 2009; Zhang and Liu 2015) implying that in the *umamit44* cytosol a N/glutamate deficiency signal is transduced regulating C flow into the flavonoid biosynthetic pathway while releasing ammonium for re-assimilation via GDH and extraplastidial availability of glutamate (Figs. 4E and 8). Changes in N/AA signaling may also explain why *umamit44* mutants continue N assimilation despite plastidial glutamate accumulation (Fig. 4A). While plant AA signal transduction pathways remain elusive, several studies have demonstrated that glutamate or other amino acids function as signaling molecules activating GLR ion channels (Qi et al. 2006; Vincill et al. 2012), thereby regulating many physiological processes including N and C metabolism (Kang and Turano 2003; Grenzi et al. 2022; Simon et al. 2023). Both GLR3.4 and GLR3.5.2 have been localized to the Arabidopsis chloroplast inner envelope, most probably with their ligand-binding domain sensing the outer/cytosolic space (Teardo et al. 2011; 2015; Simon et al. 2023). Expression of both *GLR3.4* and *GLR3.5.2* was upregulated in *umamit44* leaves (Fig. 4D), suggesting that the GLRs are required to maintain chloroplast integrity and N (and C) metabolism to, for example, accommodate extraplastidial glutamate/N needs. Further, it has been shown for GLR3.4 that GSH additionally regulates channel activity by binding to the amino-terminal domain (Green et al. 2021). It is therefore fair to speculate for *umamit44* that the changes in glutamate homeostasis and subsequent alterations in redox potential and GSH concentrations (see above; Fig. 2, E and F) may regulate GLRs and downstream oxidative signaling events (c.f. Simon et al. 2023). If GLR-mediated alterations in calcium fluxes or other regulatory mechanisms lead to the observed metabolic adjustments in the *umamit44* chloroplasts and cytosol remains to be investigated (c.f. Stephens et al. 2008; Cho et al. 2009; Vincill et al. 2012; Wudick et al. 2018).

Recent work has shown that transporters functioning in AA phloem loading are critical for source-to-sink N partitioning and plant productivity (Tan et al. 2010; Zhang et al. 2010; Zhang et al. 2015; Santiago and Tegeder 2016; Garneau et al. 2018; c.f. Rosado-Souza et al. 2023). Current studies resolved that export of glutamate (and probably other amino acids) from plastids presents an initial bottleneck for effective AA phloem loading and sink N supply. This is corroborated by the downregulation of AA phloem loader genes *AAP8* and *CAT6* (Fig. 7A; Hammes et al. 2006; Santiago and Tegeder 2016; Perchlik and Tegeder 2017), decreased level of glutamate in phloem exudates (Fig. 7C), and decreased seed protein levels (Fig. 7F) in *umamit44* plants. In addition, levels of amino acids that may be used as precursors for glutamate production outside the plastids or to reduce glutamate-induced stress within the plastids (e.g. glutamine, proline, and alanine; see above), were also severely reduced in the phloem exudate (Fig. 7C, Supplementary Table S2), suggesting that *umamit44* leaf cells rebalance AA metabolic and partitioning processes to accommodate both source and sink N requirements. But it is yet unknown, how the source cells sense AA disturbances, decide what needs to be done next, restore or adjust their AA homeostasis to a new status quo by altering physiological processes, and orchestrate modified AA availability for source and sink physiology.

Glutamate is central to plant functions and stands at the starting point of N metabolic pathways (Fig. 8). In addition, it plays a key signaling role in physiological processes including at the interface of C and N metabolism, and in the cellular responses to environmental stresses. N assimilation and glutamate synthesis occur in plastids, and the current study demonstrates that the plastidial exporter UMAMIT44 exerts regulatory control over glutamate availability within the chloroplasts, its allocation to the cytosol and its transport over long distances (Figs. 2, B and D, 3A, 7, A and C). Glutamate imbalances inside and outside the plastids seem to affect the cellular redox status and influence both N and C metabolism and sink supply (Figs. 4, A to G, 6, and 7, A to D) with negative consequences for plant growth and seed yield (Figs. 3, C and D, and 7, E and F). Nevertheless, when glutamate accumulates in plastids through decreased export, plants demonstrate a remarkable plasticity by attenuating oxidative stress through the production of other amino acids and antioxidants, and by accelerating alternative, extraplastidial pathways for glutamate synthesis. With the current and recent work in Arabidopsis and petunia on plastidial glutamate (Figs. 1 to 8) and phenylalanine (Widhalm et al. 2015) export, respectively, we are just at the infancy of understanding the kind of transporters needed to mediate chloroplast efflux (and influx) of protein or nonprotein amino acids and related compounds, and how they affect metabolic networks, metabolite levels and sink N nutrition.

Materials and methods

Subcellular localization of UMAMIT44

Several programs were used for prediction of the subcellular localization of the UMAMIT44 isoforms including Predotar (Small et al. 2004), BaCelLo (Pierleoni et al. 2006), WoLF PSORT (Horton et al. 2007), SUBA5 (Hooper et al. 2017), AtSubP (Kaundal et al. 2010), and LOCALIZER (Sperschneider et al. 2017; see Supplementary Table S1). Two UMAMIT44 isoforms seem to be synthesized by alternative translation initiation, At3g28130.2 (355 amino acids), and a shorter protein (At3g28130.1) lacking the N-terminal 89 amino acids. The open reading frame of both versions was amplified from leaf cDNA by PCR without the stop codon (for primers see Supplementary Table S3), cloned into pENTR D/TOPO (Lifetechnologies, Chicago, IL, USA) and then introduced by LR clonase recombination into the Gateway-compatible vector pB7FWG2,0 (Karimi et al. 2002; At3g28130.2) or pUB-Dest (Grefen et al. 2010; At3g28130.1) containing eGFP for C-terminal fusion. PCR reactions were performed using Phusion High-Fidelity DNA Polymerase (New England Biolabs, Frankfurt, Germany), and cloned PCR products were verified by sequencing. Using the *Agrobacterium tumefaciens*

infiltration method (Sparkes et al. 2006), UMAMIT44-GFP fusion proteins were either transiently expressed in leaf epidermal cells of *Nicotiana benthamiana* as described by Bartetzko et al. (2009; At3g28130.2), or the construct (At3g28130.1) was transferred into *Agrobacterium tumefaciens* strain GV3101 (Koncz and Schell 1986) and co-infiltration was done with GV3101::pMP90 strain harboring the p19 protein gene of tomato bushy stunt virus (Voinnet et al. 2003). Protoplasts were isolated after 3 d, and transporter-GFP localization was visualized in protoplasts or leaf cells by using a Zeiss laser scanning microscope as described (Breuers et al. 2012). Colocalization was performed using chlorophyll autofluorescence.

Plant growth and materials

Two independent Arabidopsis (*Arabidopsis thaliana*, ecotype Columbia-0) T-DNA insertion lines of *UMAMIT44* (At3g28130) were purchased from the Arabidopsis Biological Resource Center at the Ohio State University (https://abrc.osu.edu/), *umamit44-1* (SALK021827C) and *umamit44-2* (SALK099629C). The lines were screened for homozygosity and grown along with WT plants in 36-well Com-Packs (T.O. Plastics, Clearwater, MN, USA) for molecular, biochemical, and phenotypic analyses, or in single pots (100 cm^2) for photosynthetic rate measurements. Plant growth conditions used are described in Santiago and Tegeder (2016). Fully expanded source leaves (rosette leaf number 1 to 4), developing sink leaves (leaf 11 to 14), whole rosettes, and roots were collected during the vegetative growth stage at 4 wks after planting and either flash-frozen in liquid nitrogen (N) and stored at −80 °C until analysis, or directly used for phloem exudate collection, leaf chloroplast isolation, or rosette leaf area and shoot biomass measurements. For leaf area analysis, rosettes were pressed between two layers of transparent foil and imaged using a flatbed scanner followed by image processing with ImageJ2 (Rueden and Eliceiri 2019; National Institute of Health, Bethesda, MD, USA). For seed protein and yield analyses, plants were grown until maturity.

Chloroplast isolation

Leaf disks (0.9 cm diameter) were collected from source leaves (leaves 1 to 4; 1 disk per plant). Sample pools of 8 disks for at least 5 biological replicates ($n \geq 5$) were used to obtain chloroplasts with the Minute Chloroplast Isolation Kit according to the manufacturer's protocol (Invent Biotechnologies, Inc, Plymouth, MN, USA). Chlorophyll content was determined by employing specific absorption coefficients at 480, 645, and 663 nm wavelength as described (Rowan 1989) and to equalize sample concentration for AA analyses (see below). Amino acids were extracted from intact chloroplast suspensions using 80% methanol at 70 °C for 15 min, and while shaking (1,000 rpm). After 15 min centrifugation at 10,000 × *g*, the supernatant was transferred to a new tube and the pellet was re-extracted with 20% methanol. Supernatants from both extractions were combined and dried (SpeedVac concentrator; Savant Instruments, Hyderabad, India). The resulting pellet was resuspended in 160 μL of sterile double-deionized water, and 45 μL was used for high performance liquid chromatography (HPLC).

Collection of leaf phloem exudates

Phloem exudates were collected from source leaves (leaves 3 and 4) in EDTA-containing buffer for 2 h as described by Deeken et al. (2008) and Santiago and Tegeder (2016). Exudates were aliquoted (80 μL), freeze-dried, and resuspended in 33 μL of double-deionized water. The EDTA in solution was precipitated by adding 1:10 volume of 1 N HCl and incubated on ice for 30 min. Following centrifugation at 10,000 × *g* for 30 min at 4 °C, the supernatant was stored at −80 °C until analysis.

RT-PCR and RT-qPCR

Total RNA was extracted from source and sink leaves, and roots using the TRIzol Reagent (Thermo Fisher Scientific, Waltham, MA, USA) according to Chomczynski and Sacchi (1987). DNA contaminants were removed using the TURBO DNA-free™ Kit (Thermo Fisher Scientific, Waltham, MA, USA) following the manufacturer's protocol. RT-PCR was performed as described (Santiago and Tegeder 2016) and by using Moloney Murine Leukemia Virus reverse transcriptase (Thermo Fisher Scientific, Waltham, MA, USA) and *UmamiT44*-specific primers (Supplementary Table S3). RT-quantitative PCR (RT-qPCR) was done according to Zhang et al. (2010) and with an Applied Biosystems 7,500 FastThermal cycler (Foster City, CA, USA). Changes in gene expression were determined by comparing cycle threshold values with the control gene ACTIN2 (At3g18780) and *UBIQUITIN11* (At4g05050) using the $2^{-\Delta\Delta CT}$ method (Livak and Schmittgen 2001).

HPLC analysis of amino acids and GSH

Free amino acids and GSH were extracted from lyophilized leaf tissues (2 mg) according to Garneau et al. (2021). Twenty-fold diluted tissue extracts, undiluted chloroplast extracts, or undiluted leaf phloem exudates (each 45 μl) were derivatized with 4-fluoro-7-nitro-2,1,3-benzoxadiazole (NBD-F; Sigma-Aldrich, St. Louis, MO, USA) according to Aoyama et al. (2004). A standard was prepared with a commercially available AA mixture (Sigma Aldrich, St Louis, MO, USA) supplemented with arginine, glutamine, histidine, lysine, homo-serine, and reduced or oxidized GSH, and used at a final concentration of 25 μM for each N compound. HPLC analysis was performed with a Waters 2,695 separation module with column heater, autosampler, and Empower2 software (Waters, Milford, MA, USA) as previously described (Garneau et al. 2021; Lu et al. 2022). Amino acids and GSH were identified with a Waters 2,475 multi λ fluorescence detector at 470 nm wavelength excitation and 540 nm emission, and concentrations were determined by comparing sample peak areas against a standard curve.

Transport measurements in *Xenopus* oocytes

Transport studies were performed according to Zourelidou et al. (2014) and Müller et al. (2015). *UMAMIT44* cDNA (At3g28130.1) was cloned into the pOO2 vector, and transcribed cRNA was injected into oocytes of *Xenopus laevis*. As a negative control, water was used instead of *UMAMIT44* cRNA. Oocytes were incubated in Barth's solution consisting of 88 mM NaCl, 1 mM KCl, 0.8 mM $MgSO_4$, 0.4 mM $CaCl_2$, 0.3 mM $Ca(NO_3)_2$, 2.4 mM $NaHCO_3$, and 10 mM HEPES (pH 7.4) supplemented with 50 μL gentamycin at 16 °C to allow for transporter protein synthesis. Transport measurements were performed 4 d after incubation. Oocytes were injected with 50 nL of 5 mM [^{14}C]-glutamate, glutamine, proline, alanine, or glycine (American Radiochemicals, St. Louis, MO, USA), resulting in a final internal concentration of 1 mM based on the estimated oocyte total volume of 400 nL. Oocytes were incubated on ice for 2 min to permit closure of the injection site, washed and transferred to Barth's solution at 21 °C to allow for export of the respective AA. Residual amounts of the labeled AA within the oocytes were determined by scintillation counting immediately at 0 min to establish a base line, and after 30 min incubation. Depending on the AA tested, 2 to 6 independent transport experiments were performed, and 7 to 10 individual oocytes were analyzed per experiment and treatment.

Analysis of mutant growth on media containing specific amino acids

Seeds were surface-sterilized as described in Perchlik et al. (2014), stratified at 4 °C in the dark for 3 d, plated on full-strength MS medium (Murashige and Skoog 1962) containing 1% sucrose (w/v) and 0.8% agar (w/v; Phytotechnology Laboratories, Shawnee, KS, USA), and grown in the tissue culture chamber at 16-h daylength and 200 μmol photons m^{-2} s^{-1}. Day/night temperatures were set at 21° C/16 °C and 70% relative humidity. After 14 d, seedlings were transferred to MS medium supplemented with or without amino acids, specifically glutamate (50 mM Glu), glutamine (25 mM Gln), proline (25 mM Pro), aspartate (25 mM Asp), asparagine (10 mM Asn), or alanine (25 mM Ala), and grown for an additional 14 d to determine shoot dry weights.

Measurements of photosynthetic parameters

Photosynthetic rates were measured with a LI-6400XT photosynthesis system (LI-COR; Lincoln, NE, USA) using 6-wk-old plants at vegetative stage. Plants were grown at 12-h daylength for 4.5 wks to promote leaf expansion and then acclimated to 16-h daylength for 10 d. Photosynthetic rates were determined with mature source leaves at 1,000 μmol m^{-2} s^{-1} photosynthetic photon flux density (PPFD) with 90% red and 10% blue light, 25 °C leaf temperature, and 400 ppm CO_2 level.

In vivo measurements of chlorophyll-a fluorescence parameters were performed using a pulse amplitude modulated (PAM) fluorometer of the IMAGING-PAM M-Series (Effeltrich, Germany) as described by Kunz et al. (2009). WT and *keaD1* mutant plants with plastidial K^+/H^+ antiporter genes *KEA1* and *KEA2* knocked out (Kunz et al. 2014) were used as controls. *Umamit44* mutants and control plants were grown under a 16-h daylength until 15, 16, 17, or 18 d after germination at temperature and light conditions described above. Before fluorescence measurements plants were adapted for 30 min in the dark and then a light induction curve was recorded using the standard settings of the manufacturer's software at actinic light 8 (186 μmol quanta m^{-2} s^{-1}) and slow induction parameters (40 s delay, 20 s clock, and 315 s measurement time). At the start of each measurement, the ratio of variable to maximum chlorophyll a fluorescence yield (F_v/F_m; Maxwell and Johnson 2000) was calculated. NPQ was analyzed according to Bilger and Björkman (1990), and the quantum efficiency of electron flux through PSII (Φ_{PSII}) was determined following Genty et al. (1989).

Carbohydrate and protein assays

Glucose, sucrose, and starch were extracted from 3 mg lyophilized leaf tissue with 500 μL of 80% ethanol, and levels were measured using the Amplex Red Glucose/Glucose Oxidase Assay kit (Thermo Fisher Scientific, Waltham, MA, USA) based on the manufacturer's instructions and as described by Santiago and Tegeder (2017). Total soluble proteins were extracted from lyophilized leaf or dry seed tissues (2 mg) following Zhang et al. (2010). Proteins were measured with the NanoOrange protein quantitation kit (Invitrogen, Carlsbad, CA, USA) according to the manufacturer's protocol, and by using a BioTek Synergy HT microplate fluorescence reader equipped with KC4 v.3.4 software (Winooski, VA, USA) at 480 nm excitation wavelength and 590 nm emission.

Quantification of anthocyanin and other flavonoids

Flavonoid content was measured as described by Ronchi et al. (1997). Fully expanded source leaves (rosette leaf number 1 to 4) were collected, weighed, and ground in 1 mL of 1% HCl in ethanol (v/v). The extracts were centrifuged twice at 14,000 × *g* and the aqueous phase was measured spectrophotometrically at 530 and 350 nm wavelength to quantify anthocyanin and other flavonoids, respectively.

Hydrogen peroxide analysis

Hydrogen peroxide (H_2O_2) was extracted from 300 μL pulverized frozen tissue samples with 500 μL of 5% trichloroacetic acid in 50 mM sodium phosphate buffer (pH 7.4), vortexed, and centrifuged at 14,000 × *g*. The resulting supernatants were transferred to 1.5 mL microcentrifuge tubes, and hydrogen peroxide levels were quantified using the Amplex Red Hydrogen Peroxide/Peroxidase Assay Kit (ThermoFisher Scientific, Waltham, MA, USA) based on the manufacturer's directions. Fluorescence emission was measured at 590 nm with a BioTek Synergy HT microplate

fluorescence reader (Winooski, VA, USA) with KC4 v.3.4 software.

Statistical analysis

Tissue fresh and dry weights, and photosynthetic parameters were determined from individual plants. All other results were obtained from at least 4 independent tissue pools ($n \geq 4$), each consisting of 8 to 10 individual plants. Respective biological replications can be found in the figure legends. Bar graphs, box and whisker plots, as well as violin plots were made using Graphpad Prism software ver. 10.0 (GraphPad Software, Inc., La Jolla, CA, USA). Data are presented as mean ± standard deviation. To determine differences between genotypes, 1-way analysis of variance (ANOVA) and mean separation tests were performed using SigmaStat 3.0 (Systat Software Chicago, IL, USA). Small, moderate, and large statistically significant changes are specified as $^{*}P \leq 0.05$, $^{**}P \leq 0.01$, and $^{***}P \leq 0.001$, respectively. The numbers above columns indicate percent change versus the wild type. Statistical data are provided in Supplemental Data Set S1.

Accession numbers

The Arabidopsis Genome Initiative numbers for the genes mentioned in this article are as follows: *UMAMIT44* (At3g28130), *GLN1; 2* (At1g66200), *GLN1; 3* (At3g17820), *GLN2* (At5g35630), *GLU1* (At5g04140), *GLU2* (At2g41220), *GDH1* (At5g18170), *P5CS1* (At2g39800), *P5CS2* (At3g55610), *ProDH2* (At5g38710), *P5CDH* (At5g62530), *AlaAT1* (At1g17290), *AlaAT2* (At1g72330), *NFS2* (At1g08490), *GSH1* (At4g23100), *GSH2* (At5g27380), *GLR1.4* (At3g07520), *GLR3.2* (At4g35290), *GLR3.3* (At1g42540), *GLR3.4* (At1g05200), *GLR3.5.2* (At2g32390.2), *DiT2.1* (At5g64290), *CAT6* (At5g04770), *CAT7* (At3g10600), *AAP1* (At1g58360), *AAP2* (At5g09220), *AAP3* (At1g77380), *AAP4* (At5g63850), *AAP5* (At1g44100), *AAP8* (At1g10010), *CHS* (At5g13930), *FLS3* (At5g63590), *ACT2* (At3g18780), and *UBQ11* (At4g05050).

Acknowledgments

We gratefully acknowledge the help from Karolin Montag at the Heinrich-Heine University, Düsseldorf with screening 1 mutant line and the technical support from the WSU greenhouse managers Chuck Cody and Amanda Linskey. We thank Dr. Hans-Henning Kunz at the Ludwig-Maximilian University of Munich for providing the *keaD1* mutant line.

Author contributions

M.T. and S.V.T. designed the study and wrote the paper. S.V.T. and J.P.S. performed the HPLC analyses, C.P. and U.Z.H. the electrophysiological measurements and S.V.T. all other experiments. All authors read and approved the final manuscript.

Supplementary data

The following materials are available in the online version of this article.

Supplementary Table S1. Subcellular location prediction of UMAMIT44.

Supplementary Table S2. Amino acid analyses of chloroplasts, source leaves, and leaf phloem exudates.

Supplementary Table S3. Overview of primers used for analyses.

Supplementary Data Set 1. Statistical data.

Funding

This research was supported by a grant of the National Science Foundation to MT (IOS 1932661) and the German Research Foundation (DFG) SFB924 TP A08 to UZH.

Conflict of interest statement. The authors declare no conflicts of interests.

Data availability

The authors declare that all data supporting the findings of this study are available within the article and its online supplementary files.

References

Alia, Mohanty P, Matysik J. Effect of proline on the production of singlet oxygen. Amino acids. 2001:**21**(2):195–200. https://doi.org/10.1007/s007260170026

Allen DK, Libourel IG, Shachar-Hill Y. Metabolic flux analysis in plants: coping with complexity. Plant Cell Environ. 2009:**32**(9):1241–1257. https://doi.org/10.1111/j.1365-3040.2009.01992.x

Alvarez ME, Savouré A, Szabados L. Proline metabolism as regulatory hub. Trends Plant Sci. 2022:**27**(1):39–55. https://doi.org/10.1016/j.tplants.2021.07.009

Aoyama C, Santa T, Tsunoda M, Fukushima T, Kitada C, Imai K. A fully automated amino acid analyzer using NBD-F as a fluorescent derivatization reagent. Biomed Chromatogr. 2004:**18**(9):630–636. https://doi.org/10.1002/bmc.365

Arrivault S, Obata T, Szecówka M, Mengin V, Guenther M, Hoehne M, Fernie AR, Stitt M. Metabolite pools and carbon flow during C4 photosynthesis in maize: $13CO_2$ labeling kinetics and cell type fractionation. J Exp Bot. 2017:**68**(2):283–298. https://doi.org/10.1093/jxb/erw414

Awai K, Xu C, Tamot B, Benning C. A phosphatidic acid-binding protein of the chloroplast inner envelope membrane involved in lipid trafficking. Proc Natl Acad Sci. 2006:**103**(28):10817–10822. https://doi.org/10.1073/pnas.0602754103

Bartetzko V, Sonnewald S, Vogel F, Hartner K, Stadler R, Hammes UZ, Börnke F. The *Xanthomonas campestris* pv. *vesicatoria* type III effector protein XopJ inhibits protein secretion: evidence for interference with cell wall–associated defense responses. Mol Plant-Microbe Interact. 2009:**22**(6):655–664. https://doi.org/10.1094/MPMI-22-6-0655

Baxter A, Mittler R, Suzuki N. ROS as key players in plant stress signalling. J Exp Bot. 2014:**65**(5):1229–1240. https://doi.org/10.1093/jxb/ert375

Bela K, Horváth E, Gallé Á, Szabados L, Tari I, Csiszár J. Plant glutathione peroxidases: emerging role of the antioxidant enzymes in plant development and stress responses. J Plant Physiol. 2015:**176**:192–201. https://doi.org/10.1016/j.jplph.2014.12.014

Besnard J, Pratelli R, Zhao C, Sonawala U, Collakova E, Pilot G, Okumoto S. UMAMIT14 is an amino acid exporter involved in phloem unloading in *Arabidopsis* roots. J Exp Bot. 2016:**67**(22):6385–6397. https://doi.org/10.1093/jxb/erw412

Besnard J, Zhao C, Avice JC, Vitha S, Hyodo A, Pilot G, Okumoto S. *Arabidopsis* UMAMIT 24 and 25 are amino acid exporters involved in transfer of amino acids to the seed. J Exp Bot. 2018:**69**(21):5221–5232. https://doi.org/10.1093/jxb/ery302

Bilger W, Björkman O. Role of the xanthophyll cycle in photoprotection elucidated by measurements of light-induced absorbance changes, fluorescence and photosynthesis in leaves of *Hedera canariensis*. Photosynth Res. 1990:**25**(3):173–185. https://doi.org/10.1007/BF00033159

Breuers FK, Bräutigam A, Geimer S, Welzel UY, Stefano G, Renna L, Brandizzi F, Weber AP. Dynamic remodeling of the plastid envelope membranes–a tool for chloroplast envelope in vivo localizations. Front Plant Sci. 2012:**3**:7. https://doi.org/10.3389/fpls.2012.00007

Cho D, Kim SA, Murata Y, Lee S, Jae SK, Nam HG, Kwak JM. De-regulated expression of the plant glutamate receptor homolog *AtGLR3.1* impairs long-term Ca^{2+}-programmed stomatal closure. Plant J. 2009:**58**(3):437–449. https://doi.org/10.1111/j.1365-313X.2009.03789.x

Chomczynski P, Sacchi N. Single-step method of RNA isolation by acid guanidinium thiocyanate-phenol-chloroform extraction. Anal Biochem. 1987:**162**(1):156–159. https://doi.org/10.1016/0003-2697(87)90021-2

Contreras-López, O., Vidal, E. A., Riveras, E., Alvarez, J. M., Moyano, T. C., Sparks, E. E., EE Sparks, J Medina, A Pasquino, PN Benfey, GM, et al. Spatiotemporal analysis identifies ABF2 and ABF3 as key hubs of endodermal response to nitrate. Proc Natl Acad Sci. 2022:**119**(4):1–11. https://doi.org/10.1073/pnas.2107879119

Das K, Roychoudhury A. Reactive oxygen species (ROS) and response of antioxidants as ROS-scavengers during environmental stress in plants. Front Environ Sci. 2014:**2**:53. https://doi.org/10.3389/fenvs.2014.00053

D'Autréaux B, Toledano MB. ROS as signalling molecules: mechanisms that generate specificity in ROS homeostasis. Nat Rev Mol Cell Biol. 2007:**8**(10):813–824. https://doi.org/10.1038/nrm2256

Deeken R, Ache P, Kajahn I, Klinkenberg J, Bringmann G, Hedrich R. Identification of *Arabidopsis thaliana* phloem RNAs provides a search criterion for phloem-based transcripts hidden in complex datasets of microarray experiments. Plant J. 2008:**55**(5):746–759. https://doi.org/10.1111/j.1365-313X.2008.03555.x

Durand M, Brehaut V, Clement G, Kelemen Z, Macé J, Feil R, Duville G, Launay-Avon A, Paysant-Le Roux C, Lunn JE, et al. The Arabidopsis transcription factor NLP2 regulates early nitrate responses and integrates nitrate assimilation with energy and carbon skeleton supply. Plant Cell. 2023:**35**(5):1429–1454. https://doi.org/10.1093/plcell/koad025

Eisenhut M, Hoecker N, Schmidt SB, Basgaran RM, Flachbart S, Jahns P, Eser T, Geimer S, Husted S, Weber APM, et al. The plastid envelope CHLOROPLAST MANGANESE TRANSPORTER1 is essential for manganese homeostasis in *Arabidopsis*. Mol Plant. 2018:**11**(7):955–969. https://doi.org/10.1016/j.molp.2018.04.008

Facchinelli F, Weber AP. The metabolite transporters of the plastid envelope: an update. Front Plant Sci. 2011:**2**:50. https://doi.org/10.3389/fpls.2011.00050

Feinbaum RL, Ausubel FM. Transcriptional regulation of the *Arabidopsis thaliana* chalcone synthase gene. Mol Cell Biol. 1988:**8**(5):1985–1992. https://doi.org/10.1128/mcb.8.5.1985-1992.1988

Fischer K. The import and export business in plastids: transport processes across the inner envelope membrane. Plant Physiol. 2011:**155**(4):1511–1519. https://doi.org/10.1104/pp.110.170241

Forde BG, Lea PJ. Glutamate in plants: metabolism, regulation, and signalling. J Exp Bot. 2007:**58**(9):2339–2358. https://doi.org/10.1093/jxb/erm121

Garneau MG, Lu MZ, Grant J, Tegeder M. Role of source-to-sink transport of methionine in establishing seed protein quantity and quality in legumes. Plant Physiol. 2021:**187**(4):2134–2155. https://doi.org/10.1093/plphys/kiab238

Garneau MG, Tan Q, Tegeder M. Function of pea amino acid permease AAP6 in nodule nitrogen metabolism and export, and plant nutrition. J Exp Bot. 2018:**69**(21):5205–5219. https://doi.org/10.1093/jxb/ery289

Gaufichon L, Rothstein SJ, Suzuki A. Asparagine metabolic pathways in *Arabidopsis*. Plant Cell Physiol. 2016:**57**(4):675–689. https://doi.org/10.1093/pcp/pcv184

Genty B, Briantais JM, Baker NR. The relationship between the quantum yield of photosynthetic electron transport and quenching of chlorophyll fluorescence. Biochim Biophys Acta-Gen Subj. 1989:**990**(1):87–92. https://doi.org/10.1016/S0304-4165(89)80016-9

Green MN, Gangwar SP, Michard E, Simon AA, Portes MT, Barbosa-Caro J, Wudick MM, Lizzio MA, Klykov O, Yelshanskaya MV, et al. Structure of the *Arabidopsis thaliana* glutamate receptor-like channel GLR3.4. Mol Cell. 2021:**81**(15):3216–3226. https://doi.org/10.1016/j.molcel.2021.05.025

Grefen C, Donald N, Hashimoto K, Kudla J, Schumacher K, Blatt MR. A ubiquitin-10 promoter-based vector set for fluorescent protein tagging facilitates temporal stability and native protein distribution in transient and stable expression studies. Plant J. 2010:**64**(2):355–365. https://doi.org/10.1111/j.1365-313X.2010.04322.x

Grenzi M, Bonza MC, Costa A. Signaling by plant glutamate receptor-like channels: what else!. Curr Opin Plant Biol. 2022:**68**:102253. https://doi.org/10.1016/j.pbi.2022.102253

Grotewold E. The genetics and biochemistry of floral pigments. Annu Rev Plant Biol. 2006:**57**(1):761–780. https://doi.org/10.1146/annurev.arplant.57.032905.105248

Hahlbrock K, Scheel D. Physiology and molecular biology of phenylpropanoid metabolism. Annu Rev Plant Biol. 1989:**40**(1):347–369. https://doi.org/10.1146/annurev.pp.40.060189.002023

Halliwell B. Reactive species and antioxidants. Redox biology is a fundamental theme of aerobic life. Plant Physiol. 2006:**141**(2):312–322. https://doi.org/10.1104/pp.106.077073

Hammes UZ, Nielsen E, Honaas LA, Taylor CG, Schachtman DP. AtCAT6, a sink-tissue-localized transporter for essential amino acids in *Arabidopsis*. Plant J. 2006:**48**(3):414–426. https://doi.org/10.1111/j.1365-313X.2006.02880.x

Hare PD, Cress WA. Metabolic implications of stress-induced proline accumulation in plants. Plant Growth Regul. 1997:**21**(2):79–102. https://doi.org/10.1023/A:1005703923347

Hashida SN, Miyagi A, Nishiyama M, Yoshida K, Hisabori T, Kawai-Yamada M. Ferredoxin/thioredoxin system plays an important role in the chloroplastic NADP status of *Arabidopsis*. Plant J. 2018:**95**(6):947–960. https://doi.org/10.1111/tpj.14000

Heim KE, Tagliaferro AR, Bobilya DJ. Flavonoid antioxidants: chemistry, metabolism and structure-activity relationships. J Nutr Biochem.2002:**13**(10):572–584. https://doi.org/10.1016/S0955-2863(02)00208-5

Heinemann B, Hildebrandt TM. The role of amino acid metabolism in signaling and metabolic adaptation to stress-induced energy deficiency in plants. J Exp Bot. 2021:**72**(13):4634–4645. https://doi.org/10.1093/jxb/erab182

Hildebrandt TM, Nesi AN, Araújo WL, Braun HP. Amino acid catabolism in plants. Mol Plant. 2015:**8**(11):1563–1579. https://doi.org/10.1016/j.molp.2015.09.005

Hong Z, Lakkineni K, Zhang Z, Verma DPS. Removal of feedback inhibition of Δ^1-pyrroline-5-carboxylate synthetase results in increased proline accumulation and protection of plants from osmotic stress. Plant Physiol. 2000:**122**(4):1129–1136. https://doi.org/10.1104/pp.122.4.1129

Hooper CM, Castleden IR, Tanz SK, Aryamanesh N, Millar AH. SUBA4: the interactive data analysis centre for *Arabidopsis* subcellular protein locations. Nucleic Acids Res. 2017:**45**(D1):D1064–D1074. https://doi.org/10.1093/nar/gkw1041

Horton P, Park KJ, Obayashi T, Fujita N, Harada H, Adams-Collier CJ, Nakai K. WoLF PSORT: protein localization predictor. Nucleic Acids Res. 2007:**35**(Web Server):W585–W587. https://doi.org/10.1093/nar/gkm259

Hossain MA, Bhattacharjee S, Armin SM, Qian P, Xin W, Li HY, Burritt DJ, Fujita M, Tran LSP. Hydrogen peroxide priming

modulates abiotic oxidative stress tolerance: insights from ROS detoxification and scavenging. Front Plant Sci. 2015:**6**:420. https://doi.org/10.3389/fpls.2015.00420

Huang XQ, Dudareva N. Plant specialized metabolism. Curr Biol. 2023:**33**(11):R473–R478. https://doi.org/10.1016/j.cub.2023.01.057

Kang J, Turano FJ. The putative glutamate receptor 1.1 *(AtGLR1.1)* functions as a regulator of carbon and nitrogen metabolism in *Arabidopsis thaliana*. Proc Natl Acad Sci. 2003:**100**(11):6872–6877. https://doi.org/10.1073/pnas.1030961100

Karimi M, Inzé D, Depicker A. GATEWAY vectors for *Agrobacterium*-mediated plant transformation. Trends Plant Sci. 2002:**7**(5):193–195. https://doi.org/10.1016/S1360-1385(02)02251-3

Kaundal R, Saini R, Zhao PX. Combining machine learning and homology-based approaches to accurately predict subcellular localization in *Arabidopsis*. Plant Physiol. 2010:**154**(1):36–54. https://doi.org/10.1104/pp.110.156851

Kishor PK, Sangam S, Amrutha RN, Laxmi PS, Naidu KR, Rao KS, Rao S, Reddy KJ, Theriappan P, Sreenivasulu N. Regulation of proline biosynthesis, degradation, uptake and transport in higher plants: its implications in plant growth and abiotic stress tolerance. Curr Sci. 2005:**88**:424–438. https://www.jstor.org/stable/24110209

Koncz C, Schell J. The promoter of TL-DNA gene 5 controls the tissue-specific expression of chimaeric genes carried by a novel type of Agrobacterium binary vector. Mol Gen Genet. 1986:**204**(3):383–396. https://doi.org/10.1007/BF00331014

Kovinich N, Kayanja G, Chanoca A, Otegui MS, Grotewold E. Abiotic stresses induce different localizations of anthocyanins in Arabidopsis. Plant Signal Behav. 2015:**10**(7):e1027850. https://doi.org/10.1080/15592324.2015.1027850

Krouk G, Mirowski P, LeCun Y, Shasha DE, Coruzzi GM. Predictive network modeling of the high-resolution dynamic plant transcriptome in response to nitrate. Genome Biol. 2010:**11**(12):1–19. https://doi.org/10.1186/gb-2010-11-12-r123

Kunz HH, Gierth M, Herdean A, Satoh-Cruz M, Kramer DM, Spetea C, Schroeder JI. Plastidial transporters KEA1, -2, and-3 are essential for chloroplast osmoregulation, integrity, and pH regulation in *Arabidopsis*. Proc Natl Acad Sci U S A. 2014:**111**(20):7480–7485. https://doi.org/10.1073/pnas.1323899111

Kunz HH, Scharnewski M, Feussner K, Feussner I, Flügge UI, Fulda M, Gierth M. The ABC transporter PXA1 and peroxisomal β-oxidation are vital for metabolism in mature leaves of *Arabidopsis* during extended darkness. Plant Cell. 2009:**21**(9):2733–2749. https://doi.org/10.1105/tpc.108.064857

Ladwig F, Stahl M, Ludewig U, Hirner AA, Hammes UZ, Stadler R, Harter K, Koch W. Siliques Are Red 1 (SIAR1) from *Arabidopsis* acts as a bidirectional amino acid transporter that is crucial for the amino acid homeostasis of siliques. Plant Physiol. 2012:**158**(4):1643–1655. https://doi.org/10.1104/pp.111.192583

Lam HM, Hsieh MH, Coruzzi G. Reciprocal regulation of distinct asparagine synthetase genes by light and metabolites in *Arabidopsis thaliana*. Plant J. 1998:**16**(3):345–353. https://doi.org/10.1046/j.1365-313x.1998.00302.x

Lawlor DW. Carbon and nitrogen assimilation in relation to yield: mechanisms are the key to understanding production systems. J Exp Bot. 2002:**53**(370):773–787. https://doi.org/10.1093/jexbot/53.370.773

Lea US, Slimestad R, Smedvig P, Lillo C. Nitrogen deficiency enhances expression of specific MYB and bHLH transcription factors and accumulation of end products in the flavonoid pathway. Planta. 2007:**225**(5):1245–1253. https://doi.org/10.1007/s00425-006-0414-x

Lillo C, Lea US, Ruoff P. Nutrient depletion as a key factor for manipulating gene expression and product formation in different branches of the flavonoid pathway. Plant Cell Environ. 2008:**31**(5):587–601. https://doi.org/10.1111/j.1365-3040.2007.01748.x

Limami AM, Glévarec G, Ricoult C, Cliquet JB, Planchet E. Concerted modulation of alanine and glutamate metabolism in young *Medicago truncatula* seedlings under hypoxic stress. J Exp Bot. 2008:**59**(9):2325–2335. https://doi.org/10.1093/jxb/ern102

Liu Y, von Wirén N. Ammonium as a signal for physiological and morphological responses in plants. J Exp Bot. 2017:**68**(10):2581–2592. https://doi.org/10.1093/jxb/erx086

Livak KJ, Schmittgen TD. Analysis of relative gene expression data using real-time quantitative PCR and the $2^{-\Delta\Delta CT}$ method. Methods. 2001:**25**(4):402–408. https://doi.org/10.1006/meth.2001.1262

López-Millán AF, Duy D, Philippar K. Chloroplast iron transport proteins–function and impact on plant physiology. Front Plant Sci. 2016:**7**:178. https://doi.org/10.3389/fpls.2016.00178

Lu MZ, Carter AM, Tegeder M. Altering ureide transport in nodulated soybean results in whole-plant adjustments of metabolism, assimilate partitioning, and sink strength. J Plant Physiol. 2022:**269**:153613. https://doi.org/10.1016/j.jplph.2021.153613

Lynch JH, Dudareva N. Aromatic amino acids: a complex network ripe for future exploration. Trends Plant Sci. 2020:**25**(7):670–681. https://doi.org/10.1016/j.tplants.2020.02.005

Ma F, Jazmin LJ, Young JD, Allen DK. Isotopically nonstationary ^{13}C flux analysis of changes in *Arabidopsis thaliana* leaf metabolism due to high light acclimation. Proc Natl Acad Sci. 2014:**111**(47):16967–16972. https://doi.org/10.1073/pnas.1319485111

Maeda HA. Evolutionary diversification of primary metabolism and its contribution to plant chemical diversity. Front Plant Sci. 2019:**10**:881. https://doi.org/10.3389/fpls.2019.00881

Maeda H, Dudareva N. The shikimate pathway and aromatic amino acid biosynthesis in plants. Annu Rev Plant Biol. 2012:**63**(1):73–105. https://doi.org/10.1146/annurev-arplant-042811-105439

Masclaux-Daubresse C, Daniel-Vedele F, Dechorgnat J, Chardon F, Gaufichon L, Suzuki A. Nitrogen uptake, assimilation and remobilization in plants: challenges for sustainable and productive agriculture. Ann Bot. 2010:**105**(7):1141–1157. https://doi.org/10.1093/aob/mcq028

Matysik J, Alia BB, Mohanty P. Molecular mechanisms of quenching of reactive oxygen species by proline under stress in plants. Curr Sci. 2002:**82**:525–532. https://www.jstor.org/stable/24105959

Maxwell K, Johnson GN. Chlorophyll fluorescence—a practical guide. J Exp Bot. 2000:**51**(345):659–668. https://doi.org/10.1093/jexbot/51.345.659

Mehrtens F, Kranz H, Bednarek P, Weisshaar B. The *Arabidopsis* transcription factor MYB12 is a flavonol-specific regulator of phenylpropanoid biosynthesis. Plant Physiol. 2005:**138**(2):1083–1096. https://doi.org/10.1104/pp.104.058032

Meyer Y, Belin C, Delorme-Hinoux V, Reichheld JP, Riondet C. Thioredoxin and glutaredoxin systems in plants: molecular mechanisms, crosstalks, and functional significance. Antioxid Redox Signal. 2012:**17**(8):1124–1160. https://doi.org/10.1089/ars.2011.4327

Mittler R, Vanderauwera S, Gollery M, Van Breusegem F. Reactive oxygen gene network of plants. Trends Plant Sci. 2004:**9**(10):490–498. https://doi.org/10.1016/j.tplants.2004.08.009

Mittler R, Zandalinas SI, Fichman Y, Van Breusegem F. Reactive oxygen species signalling in plant stress responses. Nat Rev Mol Cell Biol. 2022:**23**(10):663–679. https://doi.org/10.1038/s41580-022-00499-2

Miyashita Y, Dolferus R, Ismond KP, Good AG. Alanine aminotransferase catalyses the breakdown of alanine after hypoxia in *Arabidopsis thaliana*. Plant J. 2007:**49**(6):1108–1121. https://doi.org/10.1111/j.1365-313X.2006.03023.x

Müller-Schüssele SJ, Wang R, Gütle DD, Romer J, Rodriguez-Franco M, Scholz M, Buchert F, Lüth VM, Kopriva S, Dörmann P, et al. Chloroplasts require glutathione reductase to balance reactive oxygen species and maintain efficient photosynthesis. Plant J. 2020:**103**(3):1140–1154. https://doi.org/10.1111/tpj.14791

Müller B, Fastner A, Karmann J, Mansch V, Hoffmann T, Schwab W, Suter-Grotemeyer M, Rentsch D, Truernit E, Ladwig F, et al. Amino acid export in developing *Arabidopsis* seeds depends on UmamiT facilitators. Curr Biol. 2015:**25**(23):3126–3131. https://doi.org/10.1016/j.cub.2015.10.038

Murashige T, Skoog F. A revised medium for rapid growth and bioassays with tobacco tissue cultures. Physiol Plant. 1962:**15**(3):473–497. https://doi.org/10.1111/j.1399-3054.1962.tb08052.x

Noctor G, Foyer CH. Ascorbate and glutathione: keeping active oxygen under control. Annu Rev Plant Biol. 1998:**49**(1):249–279. https://doi.org/10.1146/annurev.arplant.49.1.249

Noctor G, Mhamdi A, Chaouch S, Han YI, Neukermans J, Marquez-Garcia B, Queval G, Foyer CH. Glutathione in plants: an integrated overview. Plant Cell Environ. 2012:**35**(2):454–484. https://doi.org/10.1111/j.1365-3040.2011.02400.x

Oikawa K, Kasahara M, Kiyosue T, Kagawa T, Suetsugu N, Takahashi F, Kanegae T, Niwa Y, Kadota A, Wada M. Chloroplast unusual positioning1 is essential for proper chloroplast positioning. Plant Cell. 2003:**15**(12):2805–2815. https://doi.org/10.1105/tpc.016428

Peng M, Hudson D, Schofield A, Tsao R, Yang R, Gu H, Bi YM, Rothstein SJ. Adaptation of *Arabidopsis* to nitrogen limitation involves induction of anthocyanin synthesis which is controlled by the *NLA* gene. J Exp Bot. 2008:**59**(11):2933–2944. https://doi.org/10.1093/jxb/ern148

Perchlik M, Foster J, Tegeder M. Different and overlapping functions of *Arabidopsis* LHT6 and AAP1 transporters in root amino acid uptake. J Exp Bot. 2014:**65**(18):5193–5204. https://doi.org/10.1093/jxb/eru278

Perchlik M, Tegeder M. Improving plant nitrogen use efficiency through alteration of amino acid transport processes. Plant Physiol. 2017:**175**(1):235–247. https://doi.org/10.1104/pp.17.00608

Petrov V, Hille J, Mueller-Roeber B, Gechev TS. ROS-mediated abiotic stress-induced programmed cell death in plants. Front Plant Sci. 2015:**6**:69. https://doi.org/10.3389/fpls.2015.00069

Pfannschmidt T. Chloroplast redox signals: how photosynthesis controls its own genes. Trends Plant Sci. 2003:**8**(1):33–41. https://doi.org/10.1016/S1360-1385(02)00005-5

Pierleoni A, Martelli PL, Fariselli P, Casadio R. Bacello: a balanced subcellular localization predictor. Bioinformatics. 2006:**22**(14):e408–e416. https://doi.org/10.1093/bioinformatics/btl222

Pohlmeyer K, Soll J, Steinkamp T, Hinnah S, Wagner R. Isolation and characterization of an amino acid-selective channel protein present in the chloroplastic outer envelope membrane. Proc Natl Acad Sci. 1997:**94**(17):9504–9509. https://doi.org/10.1073/pnas.94.17.9504

Pratelli R, Pilot G. Regulation of amino acid metabolic enzymes and transporters in plants. J Exp Bot. 2014:**65**(19):5535–5556. https://doi.org/10.1093/jxb/eru320

Preuß A, Stracke R, Weisshaar B, Hillebrecht A, Matern U, Martens S. *Arabidopsis thaliana* expresses a second functional flavonol synthase. FEBS Lett. 2009:**583**(12):1981–1986. https://doi.org/10.1016/j.febslet.2009.05.006

Qi J, Song CP, Wang B, Zhou J, Kangasjärvi J, Zhu JK, Gong Z. Reactive oxygen species signaling and stomatal movement in plant responses to drought stress and pathogen attack. J Integr Plant Biol. 2018:**60**(9):805–826. https://doi.org/10.1111/jipb.12654

Qi Z, Stephens NR, Spalding EP. Calcium entry mediated by GLR3.3, an *Arabidopsis* glutamate receptor with a broad agonist profile. Plant Physiol. 2006:**142**(3):963–971. https://doi.org/10.1104/pp.106.088989

Qiu XM, Sun YY, Ye XY, Li ZG. Signaling role of glutamate in plants. Front Plant Sci. 2020:**10**:1743. https://doi.org/10.3389/fpls.2019.01743

Ranocha P, Dima O, Nagy R, Felten J, Corratgé-Faillie C, Novák O, Morreel K, Lacombe B, Martinez Y, Pfrunder S, et al. *Arabidopsis* WAT1 is a vacuolar auxin transport facilitator required for auxin homoeostasis. Nat Commun. 2013:**4**(1):2625. https://doi.org/10.1038/ncomms3625

Renné P, Dreßen U, Hebbeker U, Hille D, Flügge UI, Westhoff P, Weber AP. The *Arabidopsis* mutant *dct* is deficient in the plastidic glutamate/malate translocator DiT2. Plant J. 2003:**35**(3):316–331. https://doi.org/10.1046/j.1365-313X.2003.01806.x

Ricoult C, Cliquet JB, Limami AM. Stimulation of alanine amino transferase (*AlaAT*) gene expression and alanine accumulation in embryo axis of the model legume *Medicago truncatula* contribute to anoxia stress tolerance. Physiol Plant. 2005:**123**(1):30–39. https://doi.org/10.1111/j.1399-3054.2005.00449.x

Rolland N, Curien G, Finazzi G, Kuntz M, Maréchal E, Matringe M, Ravanel S, Seigneurin-Berny D. The biosynthetic capacities of the plastids and integration between cytoplasmic and chloroplast processes. Annu Rev Genet. 2012:**46**(1):233–264. https://doi.org/10.1146/annurev-genet-110410-132544

Ronchi A, Farina G, Gozzo F, Tonelli C. Effects of a triazolic fungicide on maize plant metabolism: modifications of transcript abundance in resistance-related pathways. Plant Sci. 1997:**130**(1):51–62. https://doi.org/10.1016/S0168-9452(97)00190-8

Rosado-Souza L, Yokoyama R, Sonnewald U, Fernie AR. Understanding source-sink interactions: progress in model plants and translational research to crops in controlled and field conditions. Mol Plant. 2023:**16**(1):96–121. https://doi.org/10.1016/j.molp.2022.11.015

Rowan KS. Photosynthetic pigments of algae. Cambridge: Cambridge University Press; 1989.

Rubin G, Tohge T, Matsuda F, Saito K, Scheible WR. Members of the *LBD* family of transcription factors repress anthocyanin synthesis and affect additional nitrogen responses in *Arabidopsis*. Plant Cell. 2009:**21**(11):3567–3584. https://doi.org/10.1105/tpc.109.067041

Rueden CT, Eliceiri KW. Imagej for the next generation of scientific image data. Microsc Microanal. 2019:**25**(S2):142–143. https://doi.org/10.1017/S1431927619001442

Saito K, Yonekura-Sakakibara K, Nakabayashi R, Higashi Y, Yamazaki M, Tohge T, Fernie AR. The flavonoid biosynthetic pathway in *Arabidopsis*: structural and genetic diversity. Plant Physiol Biochem. 2013:**72**:21–34. https://doi.org/10.1016/j.plaphy.2013.02.001

Santiago JP, Tegeder M. Connecting source with sink: the role of *Arabidopsis AAP8* in phloem loading of amino acids. Plant Physiol. 2016:**171**(1):508–521. https://doi.org/10.1104/pp.16.00244

Santiago JP, Tegeder M. Implications of nitrogen phloem loading for carbon metabolism and transport during *Arabidopsis* development. J Integr Plant Biol. 2017:**59**(6):409–421. https://doi.org/10.1111/jipb.12533

Sato T, Harada T, Ishizawa K. Stimulation of glycolysis in anaerobic elongation of pondweed (*Potamogeton distinctus*) turions. J Exp Bot. 2002:**53**(376):1847–1856. https://doi.org/10.1093/jxb/erf036

Schenck CA, Maeda HA. Tyrosine biosynthesis, metabolism, and catabolism in plants. Phytochem. 2018:**149**:82–102. https://doi.org/10.1016/j.phytochem.2018.02.003

Sharma S, Villamor JG, Verslues PE. Essential role of tissue-specific proline synthesis and catabolism in growth and redox balance at low water potential. Plant Physiol. 2011:**157**(1):292–304. https://doi.org/10.1104/pp.111.183210

Simon AA, Navarro-Retamal C, Feijó JA. Merging signaling with structure: functions and mechanisms of plant glutamate receptor Ion channels. Annu Rev Plant Biol. 2023:**74**(1):415–452. https://doi.org/10.1146/annurev-arplant-070522-033255

Small I, Peeters N, Legeai F, Lurin C. Predotar: a tool for rapidly screening proteomes for N-terminal targeting sequences. Proteomics. 2004:**4**(6):1581–1590. https://doi.org/10.1002/pmic.200300776

Sparkes IA, Runions J, Kearns A, Hawes C. Rapid, transient expression of fluorescent fusion proteins in tobacco plants and generation of stably transformed plants. Nat Protoc. 2006:**1**(4):2019–2025. https://doi.org/10.1038/nprot.2006.286

Sperschneider J, Catanzariti AM, DeBoer K, Petre B, Gardiner DM, Singh KB, Dodds PN, Taylor JM. LOCALIZER: subcellular localization prediction of both plant and effector proteins in the plant cell. Sci Rep. 2017:**7**(1):1–14. https://doi.org/10.1038/srep44598

Steinkamp T, Hill K, Hinnah SC, Wagner R, Röhl T, Pohlmeyer K, Soll J. Identification of the pore-forming region of the outer chloroplast envelope protein OEP16. J Biol Chem. 2000:**275**(16):11758–11764. https://doi.org/10.1074/jbc.275.16.11758

Stephens NR, Qi Z, Spalding EP. Glutamate receptor subtypes evidenced by differences in desensitization and dependence on the *GLR3.3* and *GLR3.4* genes. Plant Physiol. 2008:**146**(2):529. https://doi.org/10.1104/pp.107.108134

Stewart AJ, Chapman W, Jenkins GI, Graham I, Martin T, Crozier A. The effect of nitrogen and phosphorus deficiency on flavonol

accumulation in plant tissues. Plant Cell Environ. 2001:**24**(11): 1189–1197. https://doi.org/10.1046/j.1365-3040.2001.00768.x

Strizhov N, Ábrahám E, Ökrész L, Blickling S, Zilberstein A, Schell J, Koncz C, Szabados L. Differential expression of two *P5CS* genes controlling proline accumulation during salt-stress requires ABA and is regulated by *ABA1*, *ABI1* and *AXR2* in *Arabidopsis*. Plant J. 1997:**12**(3): 557–569. https://doi.org/10.1046/j.1365-313X.1997.00537.x

Su YH, Frommer WB, Ludewig U. Molecular and functional characterization of a family of amino acid transporters from *Arabidopsis*. Plant Physiol. 2004:**136**(2):3104–3113. https://doi.org/10.1104/pp.104.045278

Szabados L, Savouré A. Proline: a multifunctional amino acid. Trends Plant Sci. 2010:**15**(2):89–97. https://doi.org/10.1016/j.tplants.2009.11.009

Székely G, Ábrahám E, Cséplo Á, Rigó G, Zsigmond L, Csiszár J, Ayaydin F, Strizhov N, Jásik J, Schmelzer E, et al. Duplicated *P5CS* genes of *Arabidopsis* play distinct roles in stress regulation and developmental control of proline biosynthesis. Plant J. 2008:**53**(1):11–28. https://doi.org/10.1111/j.1365-313X.2007.03318.x

Tan Q, Zhang L, Grant J, Cooper P, Tegeder M. Increased phloem transport of S-methylmethionine positively affects sulfur and nitrogen metabolism and seed development in pea plants. Plant Physiol. 2010:**154**(4):1886–1896. https://doi.org/10.1104/pp.110.166389

Teardo E, Carraretto L, De Bortoli S, Costa A, Behera S, Wagner R, Schiavo FL, Formentin E, Szabo I. Alternative splicing-mediated targeting of the *Arabidopsis* GLUTAMATE RECEPTOR3.5 to mitochondria affects organelle morphology. Plant Physiol. 2015:**167**(1): 216–227. https://doi.org/10.1104/pp.114.242602

Teardo E, Formentin E, Segalla A, Giacometti GM, Marin O, Zanetti M, Schiavo FL, Zoratti M, Szabò I. Dual localization of plant glutamate receptor AtGLR3.4 to plastids and plasmamembrane. Biochim Biophys Acta-Bioenerg. 2011:**1807**(3):359–367. https://doi.org/10.1016/j.bbabio.2010.11.008

Tegeder M, Hammes UZ. The way out and in: phloem loading and unloading of amino acids. Curr Opin Plant Biol. 2018:**43**:16–21. https://doi.org/10.1016/j.pbi.2017.12.002

Tegeder M, Masclaux-Daubresse C. Source and sink mechanisms of nitrogen transport and use. New Phytol. 2018:**217**(1):35–53. https://doi.org/10.1111/nph.14876

Tegeder M, Rentsch D. Uptake and partitioning of amino acids and peptides. Mol Plant. 2010:**3**(6):997–1011. https://doi.org/10.1093/mp/ssq047

The SV, Snyder R, Tegeder M. Targeting nitrogen metabolism and transport processes to improve plant nitrogen use efficiency. Front Plant Sci. 2021:**11**:628366. https://doi.org/10.3389/fpls.2020.628366

Toyota M, Spencer D, Sawai-Toyota S, Jiaqi W, Zhang T, Koo AJ, Howe GA, Gilroy S. Glutamate triggers long-distance, calcium-based plant defense signaling. Science. 2018:**361**(6407):1112–1115. https://doi.org/10.1126/science.aat7744

Trentmann O, Mühlhaus T, Zimmer D, Sommer F, Schroda M, Haferkamp I, Keller I, Pommerrenig B, Neuhaus HE. Identification of chloroplast envelope proteins with critical importance for cold acclimation. Plant Physiol. 2020:**182**(3):1239–1255. https://doi.org/10.1104/pp.19.00947

Treves H, Küken A, Arrivault S, Ishihara H, Hoppe I, Erban A, Höhne M, Moraes TA, Kopka J, Szymanski J, et al. Carbon flux through photosynthesis and central carbon metabolism show distinct patterns between algae, C3 and C4 plants. Nat Plants. 2022:**8**(1): 78–91. https://doi.org/10.1038/s41477-021-01042-5

Vincill ED, Bieck AM, Spalding EP. Ca^{2+} conduction by an amino acid-gated ion channel related to glutamate receptors. Plant Physiol. 2012:**159**(1):40–46. https://doi.org/10.1104/pp.112.197509

Voinnet O, Rivas S, Mestre P, Baulcombe D. An enhanced transient expression system in plants based on suppression of gene silencing by the p19 protein of tomato bushy stunt virus. Plant J. 2003:**33**(5): 949–956. https://doi.org/10.1046/j.1365-313X.2003.01676.x

Wang S, Alseekh S, Fernie AR, Luo J. The structure and function of major plant metabolite modifications. Mol Plant. 2019:**12**(7): 899–919. https://doi.org/10.1016/j.molp.2019.06.001

Wang X, Qiu Z, Zhu W, Wang N, Bai M, Kuang H, Cai C, Zhong X, Kong F, Lü P, et al. The NAC transcription factors SNAP1/2/3/4 are central regulators mediating high nitrogen responses in mature nodules of soybean. Nat Commun. 2023:**14**(1):4711. https://doi.org/10.1038/s41467-023-40392-w

Weber AP, Schwacke R, Flügge UI. Solute transporters of the plastid envelope membrane. Annu Rev Plant Bio. 2005:**56**(1):133–164. https://doi.org/10.1146/annurev.arplant.56.032604.144228

Widhalm JR, Gutensohn M, Yoo H, Adebesin F, Qian Y, Guo L, Jaini R, Lynch JH, McCoy RM, Shreve JT, et al. Identification of a plastidial phenylalanine exporter that influences flux distribution through the phenylalanine biosynthetic network. Nat Commun. 2015:**6**(1): 8142. https://doi.org/10.1038/ncomms9142

Wudick MM, Michard E, Oliveira Nunes C, Feijó JA. Comparing plant and animal glutamate receptors: common traits but different fates? J Exp Bot. 2018:**69**(17):4151–4163. https://doi.org/10.1093/jxb/ery153

Xu G, Fan X, Miller AJ. Plant nitrogen assimilation and use efficiency. Annu Rev Plant Biol. 2012:**63**(1):153–182. https://doi.org/10.1146/annurev-arplant-042811-105532

Xu D, Sanden NCH, Hansen LL, Belew ZM, Madsen SR, Meyer L, Jørgensen ME, Hunziker P, Veres D, Crocoll C, et al. Export of defensive glucosinolates is key for their accumulation in seeds. Nature. 2023:**617**(7959):132–138. https://doi.org/10.1038/s41586-023-05969-x

Xu Y, Wieloch T, Kaste JA, Shachar-Hill Y, Sharkey TD. Reimport of carbon from cytosolic and vacuolar sugar pools into the Calvin–Benson cycle explains photosynthesis labeling anomalies. Proc Natl Acad Sci. 2022:**119**:1–8. https://doi.org/10.1073/pnas.2121531119

Yoshiba Y, Kiyosue T, Katagiri T, Ueda H, Mizoguchi T, Yamaguchi-Shinozaki K, Wada K, Harada Y, Shinozaki K. Correlation between the induction of a gene for Δ^1-pyrroline-5-carboxylate synthetase and the accumulation of proline in *Arabidopsis thaliana* under osmotic stress. Plant J. 1995:**7**(5): 751–760. https://doi.org/10.1046/j.1365-313X.1995.07050751.x

Yuan H, Pawlowski EG, Yang Y, Sun T, Thannhauser TW, Mazourek M, Schnell D, Li L. Arabidopsis ORANGE protein regulates plastid pre-protein import through interacting with Tic proteins. J Exp Bot. 2021:**72**(4):1059–1072. https://doi.org/10.1093/jxb/eraa528

Zhang X, Abrahan C, Colquhoun TA, Liu CJ. A proteolytic regulator controlling chalcone synthase stability and flavonoid biosynthesis in *Arabidopsis*. Plant Cell. 2017:**29**(5):1157–1174. https://doi.org/10.1105/tpc.16.00855

Zhang L, Garneau MG, Majumdar R, Grant J, Tegeder M. Improvement of pea biomass and seed productivity by simultaneous increase of phloem and embryo loading with amino acids. Plant J. 2015:**81**(1):134–146. https://doi.org/10.1111/tpj.12716

Zhang X, Liu C. Multifaceted regulations of gateway enzyme phenylalanine ammonia-lyase in the biosynthesis of phenylpropanoids. Mol Plant. 2015:**8**(1):17–27. https://doi.org/10.1016/j.molp.2014.11.001

Zhang L, Tan Q, Lee R, Trethewy A, Lee YH, Tegeder M. Altered xylem-phloem transfer of amino acids affects metabolism and leads to increased seed yield and oil content in *Arabidopsis*. Plant Cell. 2010:**22**(11):3603–3620. https://doi.org/10.1105/tpc.110.073833

Zhang B, Zhang C, Liu C, Jing Y, Wang Y, Jin L, Yang L, Fu A, Shi J, Zhao F, et al. Inner envelope CHLOROPLAST MANGANESE TRANSPORTER 1 supports manganese homeostasis and phototrophic growth in *Arabidopsis*. Mol Plant. 2018:**11**(7):943–954. https://doi.org/10.1016/j.molp.2018.04.007

Zhao C, Pratelli R, Yu S, Shelley B, Collakova E, Pilot G. Detailed characterization of the UMAMIT proteins provides insight into their evolution, amino acid transport properties, and role in the plant. J Exp Bot. 2021:**72**(18):6400–6417. https://doi.org/10.1093/jxb/erab288

Zourelidou M, Absmanner B, Weller B, Barbosa IC, Willige BC, Fastner A, Streit V, Port SA, Colcombet J, van Bentem SF, et al. Auxin efflux by PIN-FORMED proteins is activated by two different protein kinases, D6 PROTEIN KINASE and PINOID. Elife. 2014:**3**: e02860. https://doi.org/10.7554/eLife.02860